Detrital zircon U–Pb ages of the Proterozoic metaclastic-sedimentary rocks in Hainan Province of South China: New constraints on the depositional time, source area, and tectonic setting of the Shilu Fe–Co–Cu ore district

Zhilin Wang [a,b], Deru Xu [a,*], Guocheng Hu [a,c], Liangliang Yu [a,c], Chuanjun Wu [a,d], Zhaochong Zhang [e], Jianxin Cai [d], Qiang Shan [a], Maozhou Hou [a,c], Huayong Chen [a]

[a] Key Laboratory of Mineralogy and Metallogeny, Guangzhou Institute of Geochemistry, Chinese Academy of Sciences, Guangzhou 510640, China
[b] School of Geosciences and Info-Physics, Central South University, Changsha 410083, China
[c] University of Chinese Academy of Sciences, Beijing 100049, China
[d] Laboratory of Oceanological Geology, South China Sea Institute of Oceanology, Chinese Academy of Sciences, Guangzhou 510301, China
[e] China University of Geosciences, Beijing 100083, China

ABSTRACT

The Shilu Fe–Co–Cu ore district, located at Hainan Province of South China, is well known for high-grade hematite-rich Fe ores and also two Precambrian host successions, i.e. the Shilu Group and the overlying Shihuiding Formation. This district has been interpreted as a banded iron formation (BIF) deposit-type, but its depositional time, source area and depositional setting have been in debate due to poor geochronological work. Detrital zircon U–Pb dating aided by cathodoluminescence imaging has been carried out on both the Shilu Group and Shihuiding Formation. Most of the zircon grains from both the successions are subrounded to rounded in morphology and have age spectra between 2000 Ma and 900 Ma with two predominant peaks at ca. 1460–1340 Ma and 1070 Ma, and three subordinate peaks at ca. 1740–1660 Ma, 1220 Ma and 970 Ma. The similar age distribution suggests the same depositional system for both successions. Linked to the geological and paleontological signatures, the Shihuiding Formation is better re-interpreted as the top, i.e. Seventh member of the Shilu Group, rather than a distinct Formation. The youngest statistical zircon age peaks for both successions, i.e. ca. 1070–970 Ma may define the maximum depositional time of the Shilu Group and interbedded BIFs. At least two erosional sources are required for deposition of the studied detrital zircons, with one proximal to provide the least abraded zircons and the other distal or recycled to offer the largely abraded zircons. The predominance of rounded or subrounded zircons over angular zircons probably implies a relatively stable tectonic setting during deposition. Given the Precambrian tectonics of Hainan Island, a retro-arc foreland basin is proposed for the deposition of the Shilu Group and interbedded BIFs. In comparison with those from the South China and other typical Grenvillian orogens, the detrital zircon age populations reveal that Hainan Island had crystalline basement similar to neither the Yangtze nor the Cathaysia Blocks. Combined with the tectonothermal events, we propose that Hainan Island was independent of South China at least before the late Ordovician and most likely attached or close to northwestern Laurentia before the breakup of Rodinia.

© 2015 Elsevier Ltd. All rights reserved.

1. Introduction

In the last two decades, the development of the accepted Precambrian successions in Hainan Province (Hainan Island) of South China by Chinese geoscientists depended mainly on petrographic, sedimentological and stratigraphic analyses, and rarely on geochronologic data (e.g., Zhang et al., 1990, 1992; Wang et al., 1991; Ma et al., 1997). Hereby, they are roughly classified into the Paleo- to Mesoproterozoic Baoban Group, the Meso- to Neoproterozoic Shilu Group and the Sinian (late Neoproterozoic) Shihuiding Formation (HBGMR, 1997). The time of deposition for these Precambrian successions has not been well-constrained and thus, the resulting depositional settings and potential

provenances for these successions are still enigmatic (for a comprehensive review see: Xu et al., 2013). This also is in part due to the poor exposure, as well as the multistage, polyphase deformation and metamorphism up to amphibolite or even granulite facies masking the nature of the protoliths (Wang et al., 1991; Ma et al., 1997; Xu et al., 2009).

The upper intercept age on concordia plot by conventional zircon U–Pb method (Ma et al., 1997), together with the magmatic zircon crystallization age of the Mesoproterozoic granites emplaced within the Baoban Group (Xu et al., 2006; Li et al., 2002), suggest a maximum depositional time at ca. 1800 Ma and a minimum depositional time at ca. 1430 Ma for the Baoban Group. A spreading back-arc or interarc basin associated with Paleo- to Mesoproterozoic rifting has been proposed for this Group (Xu et al., 2002). The time of deposition and tectonic setting of both the Shilu Group and overlying Shihuiding Formation have been subject of considerable debate (e.g., Zhao and Cawood, 2012), in part because both successions are of limited geographical extent in the Shilu area of Hainan Island with poor exposure which complicates the correlation of successions at the regional scale, and also because they host the Shilu Fe–Co–Cu ore district, the genesis of which has been controversial. Based on the discovery of algal megafossils such as *Chuaria*Walcott and *Tawuia dalensis* Hofmann, and the Sm–Nd isochron ages for hematite-rich Fe-ores in the Shilu district, the Shilu Group and Shihuiding Formation were previously interpreted as early- to middle Neoproterozoic and late Neoproterozoic successions, respectively (Zhang et al., 1990, 1992; Yao et al., 1999). A marine retro-arc foreland basin setting associated with the Grenvillian orogeny for the deposition of both successions was presumed by Xu et al. (2007a, 2015). However, Li et al. (2008a), using SHRIMP U–Pb zircon dating, suggested an age of ca. 1440–1430 Ma for deposition of the Shilu Group in a rift environment, and an age of ca. 1200–1000 Ma for the Shihuiding Formation in a foreland basin, rather than Neoproterozoic as suggested previously by Zhang et al. (1990, 1992). A Sinian, or Cambrian to Ordovician, or Devonian to Carboniferous age for deposition of both the Shilu Group and the Shihuiding Formation was also put forward by SCISTCAS (1986), based on both the whole rock Rb–Sr isochron ages and the fauna or flora (micro)fossils. Given the uncertainties regarding depositional times and settings of the host rocks, there has been considerable debate as to whether the ore metals Fe, Co and Cu were derived from the Shilu Group, whether the mineralizing event was coeval with the deposition of the Shilu Group, and what was the unambiguous mechanism that led to the formation of such large-scale, hematite-rich Fe–Co–Cu ore district which recently has been interpreted as a banded iron formation (BIF) deposit-type (Xu et al., 2013, 2014a).

In order to resolve these debates, it is necessary to substantiate certain critical aspects of ore genesis of the Shilu district and discriminate among various genetic models. Detrital zircon analysis offers a way to resolve these questions (Nelson, 2001), as zircon has the ability to withstand the effects of weathering, erosion, abrasion, and post-crystallization alteration, can survive multiple episodes of transportation, diagenesis, and metamorphism up to amphibolite facies, and has an inherently stable U–Pb isotopic system (Fedo et al., 2003). The age distribution of detrital zircon populations in (meta)sedimentary successions has been successfully used as a powerful proxy to constrain both the provenance characteristics and maximum depositional ages of clastic sedimentary rocks, to establish spatio-temporal connections among different stratigraphic successions, and to test or clarify the affiliation of different blocks or microcontinents, and thereby to unravel tectonic histories and paleogeographic reconstructions of paleocontinents or terranes, which is a key component of research into geodynamics of basin formation and orogenic processes (e.g., Gerdes and Zeh, 2006; Zhao et al., 2011; Cawood et al., 2013a; May et al., 2013; Wang et al., 2014b). By means of both SHRIMP II and LA-ICP-MS techniques coupled with cathodoluminescence (CL) imaging, this paper presents U–Pb analyses of detrital zircon from the Shilu Group and overlying Shihuiding Formation in the Shilu district. The detrital zircon gathered from these successions shows various extents of abrasion and characteristic age populations, and hence, can be used to interpret erosional provenance and depositional settings. More importantly, the youngest zircons help to pinpoint the maximum depositional time of the studied successions, which in turn provides useful information not only for genesis of the Shilu district and its association with sedimentation of the host rocks but also for correlation of the Shilu Group with the Shihuiding Formation. Moreover, the determinations of the depositional times of the stratigraphic successions have implications for understanding the relationship between Hainan Island and the South China, and their positions in Laurentia or Gondwana during the assembly and break-up of Rodinia (e.g., Li et al., 2008b; Zhao and Cawood, 2012).

2. Geological setting

South China comprises the Yangtze Block in the northwest and the Cathaysia Block in the southeast (Fig. 1a). Both continental blocks are separated by a series of major faults and have different crystalline basements and tectonic histories (Wang et al., 2007a, 2010a, 2012a, 2013a; Li et al., 2008b, 2009a; Shu et al., 2011; Zhang et al., 2014). Hainan Island, an epicontinental-type island, is located on the north margin of the South China Sea and generally regarded as the southwestern extent of the Cathaysia Block (Li et al., 1995, 2002, 2008b; Wang et al., 2013a). Because of its unusual tectonic setting (Xu et al., 2013), i.e. situated at the intersection of the Eurasian plate, Indian-Australian plate and Pacific plate, likely Hainan Island underwent at least four tectonothermal events in the late Meso- to early Neoproterozoic Grenvillian, Early Paleozoic Pan-African or Caledonian, Triassic Indosinian, and Jurassic–Cretaceous Yanshanian (Wang et al., 2013a; Xu et al., 2015).

Hainan Island (Fig. 1b) comprises mostly the Hercynian-Indosinian (ca. 300–200 Ma) and Yanshanian (175–65 Ma) granites, and the late Cretaceous and Cenozoic volcanic rocks. The Paleozoic successions occur as isolated units dispersed over the island. Precambrian strata are relatively rare and mostly outcrops in the western Island (Fig. 1b and c), and include the Baoban Group, the Shilu Group and the Shihuiding Formation in ascending stratigraphic order (Fig. 2). The Baoban Group, as the oldest stratum in Hainan Island, comprises migmatitic gneisses, plagioclase–amphibole gneisses and quartz–muscovite schists with greenschist to amphibolite grade metamorphism (Wang et al., 1991; Ma et al., 1997), which had been intruded by the Mesoproterozoic granitoids of ca. 1450–1430 Ma (Li et al., 2002, 2008a; Xu et al., 2006). However, the contact relationship between the Baoban Group and the overlying Shilu Group has been ambiguous due to the thick Quaternary cover. The Shilu Group, as the second oldest succession, is a suite of shallow marine, siliciclastic rocks and sedimentary carbonates with generally low-grade metamorphism of greenschist facies. This succession can be subdivided into six members (Fig. 2). The First, Third, Fourth and Fifth members primarily comprise schists and phyllites with rare interbeds of quartzites, and the Second member consists of crystallized dolostones locally with skarnization. The Sixth member that largely hosts the Fe– and Co–Cu ores is dominated by pyroxene–amphibole-rich rocks and banded or impure dolostones, with multiple interbeds of schists, phyllites or quartzites. Algal megafossils likely of early Neoproterozoic age, such as *Churia*, *Shouhsienia*, and *Taiuia*,
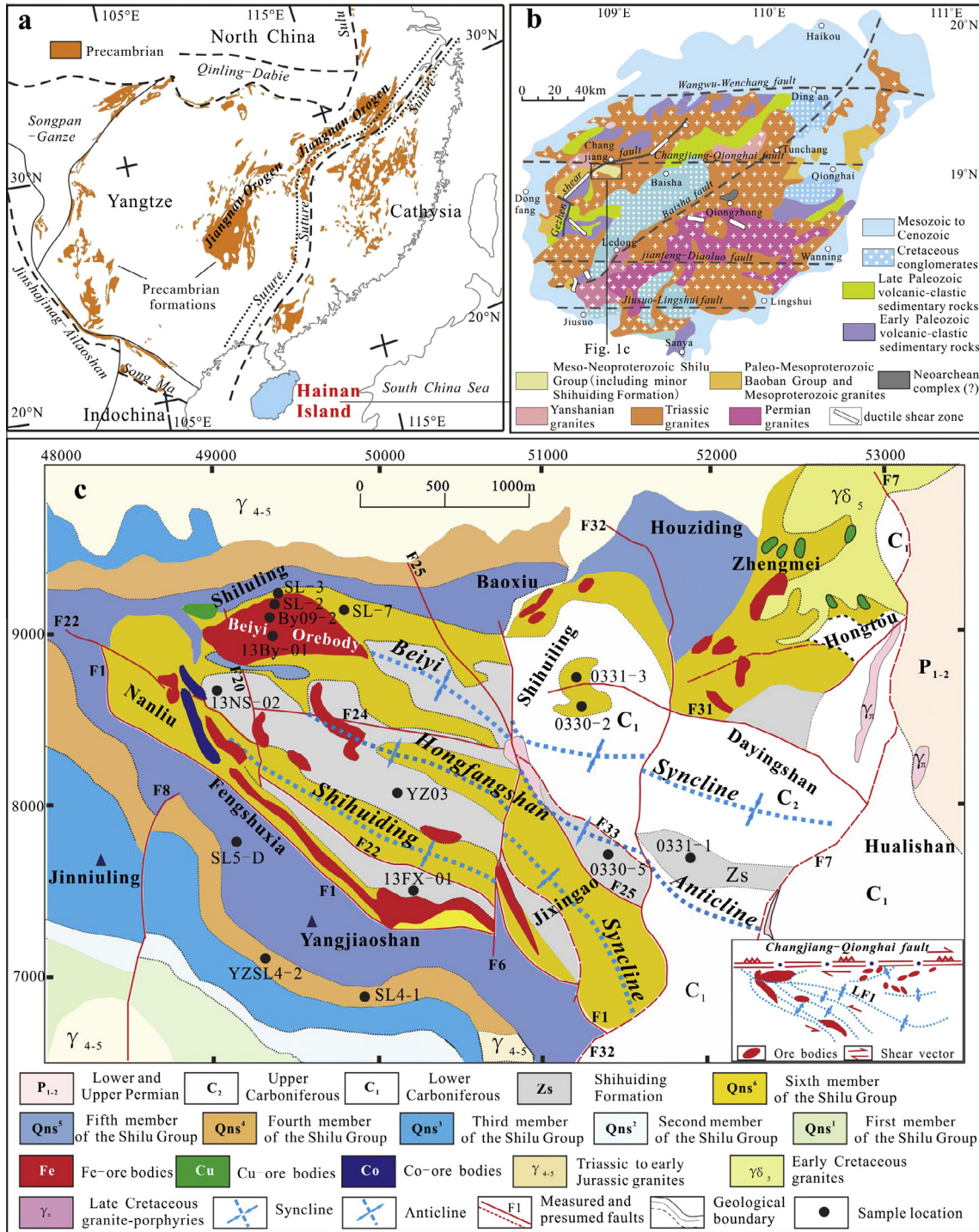
Fig. 1. (a) Tectonic framework of South China (modified after Li et al., 2002), (b) simplified map showing the main stratigraphic and magmatic units of Hainan Island (modified from Xu et al., 2013), and (c) geological sketch map of the Shilu Fe–Co–Cu ore district (modified from Xu et al., 2013). Sampling sites are shown by solid circles in (c).

have been identified from dark phyllites of the Sixth member (Zhang et al., 1990). The ~125 m thick Shihuiding Formation (Fig. 2) is a suite of terrigenous siliciclastic rocks containing depositional structures indicative of neritic-littoral deposition (Yao et al., 1999). Its lower section consists mainly of interbedded phyllites and quartz sandstones, locally with the occurrence of thin Fe–Mn ore layers. The middle section comprises mudstones, siltstones and ferruginous sandstones, of which the mudstone layers contain macroscopic algal fossils, such as *Chuaria*, *Shouhsiensia*, and

Tachymacrus (Yao et al., 1999). The upper section is composed of Fe-bearing or Fe-barren quartzites intercalated with minor sandy phyllites. SCISTCAS (1986) suggested that the Shihuiding Formation was in unconformable contact with the underlying Shilu Group, based on the presence of basal conglomerates. However, these conglomerates were subsequently designated as the Lower Carboniferous sediments (Fang et al., 1992). Our latest field investigations together with the previous work (Zhang et al., 1990) have shown that the Shihuiding Formation is indeed in fault

Time	Stratum		Local symbol	Lithology and assemblage	Histogram	Sampling	Sedimentary facies	Structural style	Metamorphic facies
Late (?) Neoproterozoic	Shihuiding Formation		Zs	Quartzose sandstones and siltstones, and phyllites interlayered with thin Fe–Mn ore beds, with thickness about 125 m	Fe Mn	YZ–03 13FX–01 13NS–02 0330–5 0331–1	Slope–neritic	Drape fold and deposited in foreland basin?	Low greenschist facies
							Fault or conformable?		
Early to Middle Neoproterozoic (?)	Shilu Group	Sixth member	Qns⁶	**Main lithostratigraphic unit hosting Fe– and Co–Cu ores** Barren, upper segment: dolostones, pelitic or carbonaceous dolostones, limestones and pyroxene–amphibole-rich rocks intercalated with slates or phyllites, containing *Chuaria-Tawuia* fossils, with thickness about 150–300 m	Fe, Fe, Fe, Co/Cu	SL-3 SL-7 By09-2 SL-2 13By-01	Neritic–thalassic	Deposited in retro-arc foreland basin?	Greenschist to amphibolite facies
				Middle segment, the main Fe-ore hosting unit: pyroxene–amphibole-rich rocks, banded or impure dolostones, and ferruginous phyllites and sandstones, locally with occurrences of gypsum, barite and jaspilite, interbedded with multilayer amphibolitic- and quartz itabirites or hematite-rich ore beds with thickness 50–400 m		0330-2 0331-3	Neritic–lagoon / Neritic–thalassic		
		Fifth member	Qns⁵				Neritic		Greenschist facies
		Fourth member	Qns⁴	Lower segment, the Co–Cu ore hosting unit: banded or impure dolostones, dolostones and pyroxene–amphibole-rich rocks intercalated with quartz–sericite schists, with thickness about 0–140 m		SL5-D		Controlled by the NW-trending synclinorium	Greenschist facies
		Third member	Qns³			SL4-1 YZSL4-2	Neritic–littoral		Greenschist facies
		Second member	Qns²	Quartz–sericite schists intercalated with silicious rocks, with thickness more than 450 m			Neritic–thalassic	Folded layer structure due to the NW-trending compression, shear and plastic flow	Greenschist to amphibolite facies
		First member	Qns¹	Quartzites intercalated with quartz–sericite schists and phyllites, with thickness about 80–140 m			Neritic		Greenschist facies
				Quartz–sericite schists intercalated with phyllites and quartz schists, with thickness about 300 m			*Unconformable*		
Paleo-Mesoproterozoic	Banban Group	Ewenling Formation	Che	Marbles with serpentinization, hortonolite, tremolite and diopside alteration, with thickness between 15 m and 100 m	γ Pt₂		Neritic	Deposited in back-arc or inter-arc basin?	High greenschist to amphibolite facies
				Andalusite-bearing quartz–sericite schists, muscovite–quartz schists, with thickness more than 900 m					
		Gezhencun Formation	Chg	Quartz–mica (sericite, muscovite) schists and mica–quartz schists intercalated with quartzites and graphite ore beds, emplaced by the Mesoproterozoic granites (γPt₂), with thickness of 420-1120 m	γ Pt₂		Neritic–littoral	Controlled by NE–SW-trending Gezhen brittle-ductile shear zone	
				Biotite plagio-gneisses, amphibolitic gneisses and migmatitic gneisses intercalated with minor biotite–plagioclase leptynites and leptites, emplaced by the Mesoproterozoic granites (γPt₂), with thickness of more than 250 m and upper to 2400 m	ca.1450-1430 Ma		Neritic	Supersposed shear structures	High amphibolite to granulite facies

Fig. 2. Simplified stratigraphic column of the Shilu mining district and its peripheral regions in the western Hainan Island, South China (after Xu et al., 2014a). This figure also indicates sampling levels and related lithological descriptions on selected samples.

contact with the Shilu Group (Fig. 3a–c). Therefore, Zhang et al. (1990) and Xu et al. (2009) have re-interpreted the Shihuiding Formation as the top, i.e. the Seventh member of the Shilu Group.

The Shilu Fe–Co–Cu ore district is situated in the western Hainan Province and has an area of ∼77 km² (Fig. 1b and c). The roughly EW-trending regional Changjiang-Qionghai deep fault zone passes through to the north of the Shilu district and the NE-trending Gezhen shear fault cuts through the western part of the district (Fig. 1b). The Shilu district comprises forty-one Fe orebodies, as well as seventeen Co- and forty-one Cu orebodies (Xu et al., 2013, 2014a). Metalliferous ores of economic significance discovered so far are only located in the Shilu Group. Both the Shilu Group and the Shihuiding Formation lie in a NW-trending synclinorium comprising a series of minor folds with the same strike (Xu et al., 2013). Consequently, the Fe– and Co–Cu ores generally occur as stratiform or stratiform-like bodies trending along troughs and/or transitional zones from limbs to troughs of the synclinorium. The Co–Cu ores typically are located about 30–60 m below the Fe-ore horizons (Xu et al., 2013). Voluminous Permian to early Jurassic granites and Cretaceous mafic to felsic dikes have also been intruded into or around the Shilu district (Fig. 1c).

3. Sample preparation and analytical methods

To compare the age spectra of the detrital zircons in the Shilu Group with that in the Shihuiding Formation, and thereby to track the nature of the source terrains and to evaluate the depositional setting, a total of fifteen samples were collected from the Shilu district (Fig. 1c). Among these, ten samples were collected from the Fourth, Fifth, and Sixth members of the Shilu Group, and the others from the Shihuiding Formation. Fig. 2 shows the sample locations. These samples include ferrugineous quartz sandstone, quartzite, mica (muscovite, biotite)-rich quartzite, quartz–mica schist, phyllite, pyroxene–amphibole-rich rock, Fe-rich ore and Fe-poor ore. Because the former five are common rocks, herein we only introduce the latter three rock types. The pyroxene–amphibole-rich rocks (Xu et al., 2013, 2015), as the main host rocks of Fe ores, are often in immediate contact with the hematite-rich Fe orebodies, and/or occur as off-white bands alternating with Fe-oxide-rich bands. This type rocks are characterized by lepidoblastic–granoblastic, nematoblastic, blastoclastic and/or rotary textures, as well as augen, banded, gneissic and schistose structures. Mineralogically, they comprise alternating actinolite + diopside ± tremolite ± K-feldspar bands with K-feldspar + quartz + sericite ± chlorite bands. Fe-rich ores (i.e. quartz itabirites; Xu et al., 2014a) are the main type of Fe-ores in the Shilu district. Mineralogically, they are dominated by hematite and quartz with minor magnetite, barite, garnet and anhydrite, with lepidoblastic, porphyroblastic, blastopsammitic and blastooolitic textures, and banding, laminated or blastobedding, and augen structures. Fe-poor ores (i.e. amphibolitic itabirites; Xu et al., 2013), characterized by 20–40 wt.% total FeO contents, are interbedded with the Fe-rich ore beds, or occur as the transitional zone between the pyroxene–amphibole-rich rocks and the Fe-rich ore beds. They comprise alternating black, millimeter- to tens of meter-scale Fe-oxide
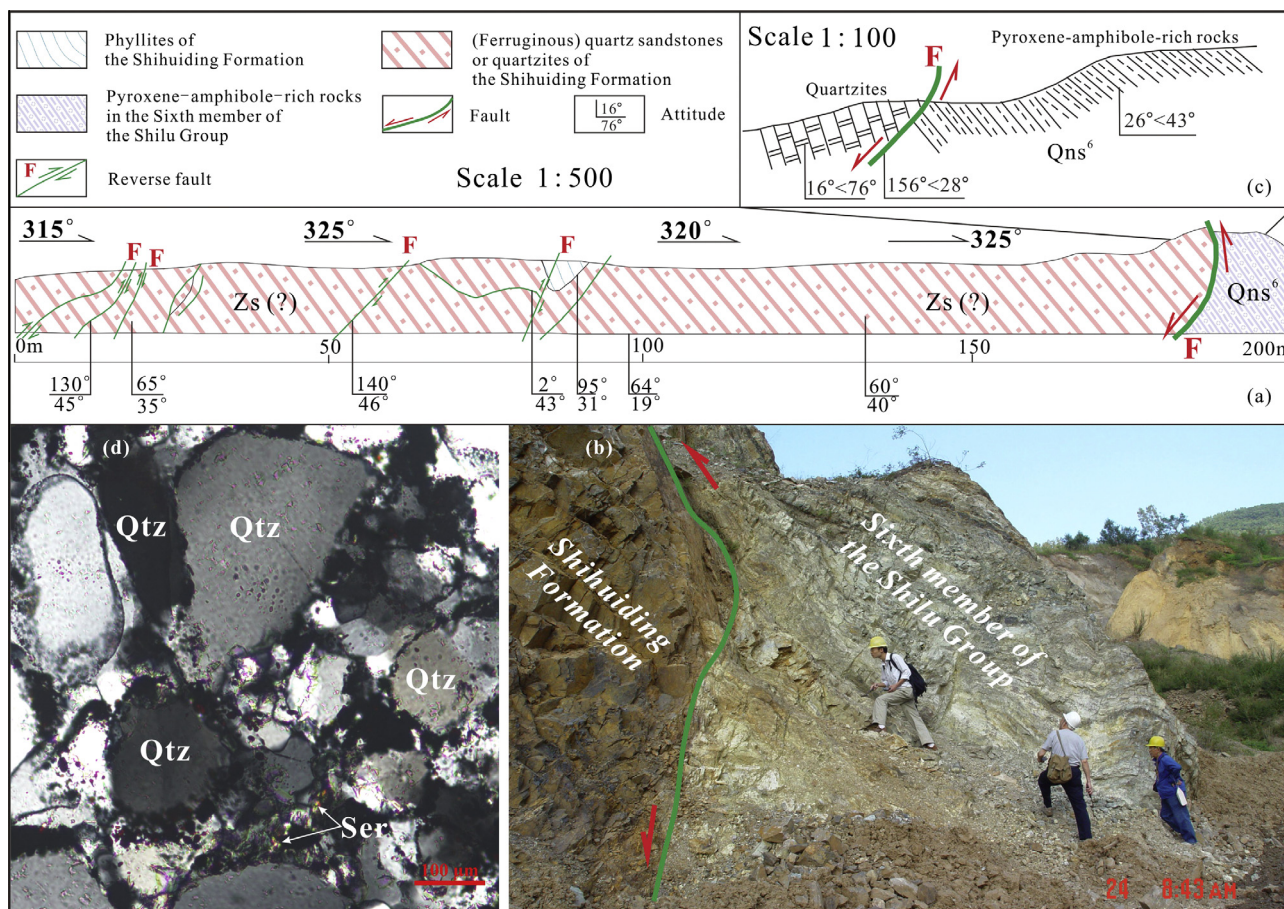
Fig. 3. Cross sections and field photograph (a–c) showing a fault contact between the Shilu Group and overlying Shihuiding Formation, and microphotograph (d) suggesting a low-grade greenschist-facies metamorphism for sandstones from the Shihuiding Formation, crossed nicols. Men in (d) represent size. Qtz = quartz, Ser = sericite.

(magnetite, hematite) + quartz bands with calc-silicate bands. The latter comprise fine- to middle-grained actinolite ± diopside ± tremolite bands alternated with fine- to medium-grained epidote ± chlorite bands and coarse-grained garnet bands.

After conventional magnetic and heavy liquid separation techniques, crushed zircon grains were handpicked under a binocular microscope, mounted in epoxy disks, polished to expose their internal structures, and then dated using a Sensitive High-Resolution Ion Microprobe (SHRIMP II) at Beijing SHRIMP Center of the Chinese Academy of Geological Sciences (Beijing). Detailed procedures followed those described in Williams et al. (1996). Both optical photomicrographs and cathodoluminescent (CL) images were taken as a guide to selection of U–Pb dating spots. The mounts were vacuum-coated with a ~500 nm layer of high-purity gold. Inter-element fractionation in the ion emission of zircon was corrected using standard TEM (417 Ma). U–Th–Pb isotope ratios and absolute abundances were determined relative to the SL13 standard zircon (572 Ma). The common Pb correction was made based on ^{204}Pb counts. Data reduction was carried out using the Squid v. 1.02 and Isoplot/Ex v. 2.49 programs (Ludwig, 2001a, 2001b).

In order to be as representative of the overall detrital zircon population as possible and to reduce the probability of missing a provenance component, i.e. to ensure the required number of measured grains (Fedo et al., 2003), we additionally conducted U–Pb dating on detrital zircon grains from the corresponding sample mounts for SHRIMP II analysis using LA-ICP-MS coupled with a Resonetics RESolution M-50 (193 nm ArF excimer) laser system in the State Key Laboratory of Isotope Geochemistry, Guangzhou

Institute of Geochemistry, Chinese Academy of Sciences. The LA-ICP-MS allows for quantitative analysis within a reasonable time frame and cost (Fedo et al., 2003). Sample mounts were placed in a special-designed double volume sample cell flushed with Ar and He. Laser ablation was operated at a constant energy (between 80 and 81 mJ/cm^2) at 10 Hz, with a spot diameter of 31 μm. The ablated material was carried by the He–Ar gas via a custom-made Squid system to homogenize the signal to the ICP-MS. Each block of five unknowns was bracketed by analysis of standards. Off-line selection and integration of background and analyzed signals, and time-drift correction and quantitative calibration for trace element analyses and U–Pb dating were performed by an in-house program ICPMSDataCal. External standard glass NIST SRM 610 and standard zircon Temora were used for external calibration. Twenty-nine Si was used as the internal standard. Common Pb was corrected using an excel programme ComPbCorr#3_17 (Andersen, 2002). Concordia diagrams and weighted mean calculations were made using Isoplot/Ex v. 3.

Uncertainties on individual analyses from both the above-mentioned methods are reported at 1σ level and mean ages for pooled ^{206}Pb/^{238}U and ^{207}Pb/^{206}Pb results are quoted at 95% confidence level. In the following analysis, ^{206}Pb/^{238}U ages are used for zircon grains with ages <1000 Ma whereas ^{207}Pb/^{206}Pb ages for the older ones. This is in that the ^{207}Pb/^{206}Pb ages become increasingly imprecise below <1000 Ma due to the change of the concordia slope (Gerdes and Zeh, 2006), whereas that ^{206}Pb/^{238}U ages are more reliable in younger grains due to the low accumulation of ^{207}Pb in younger zircons. The results with >10% or <−10% discordance were excluded when interpreting the detrital zircon ages
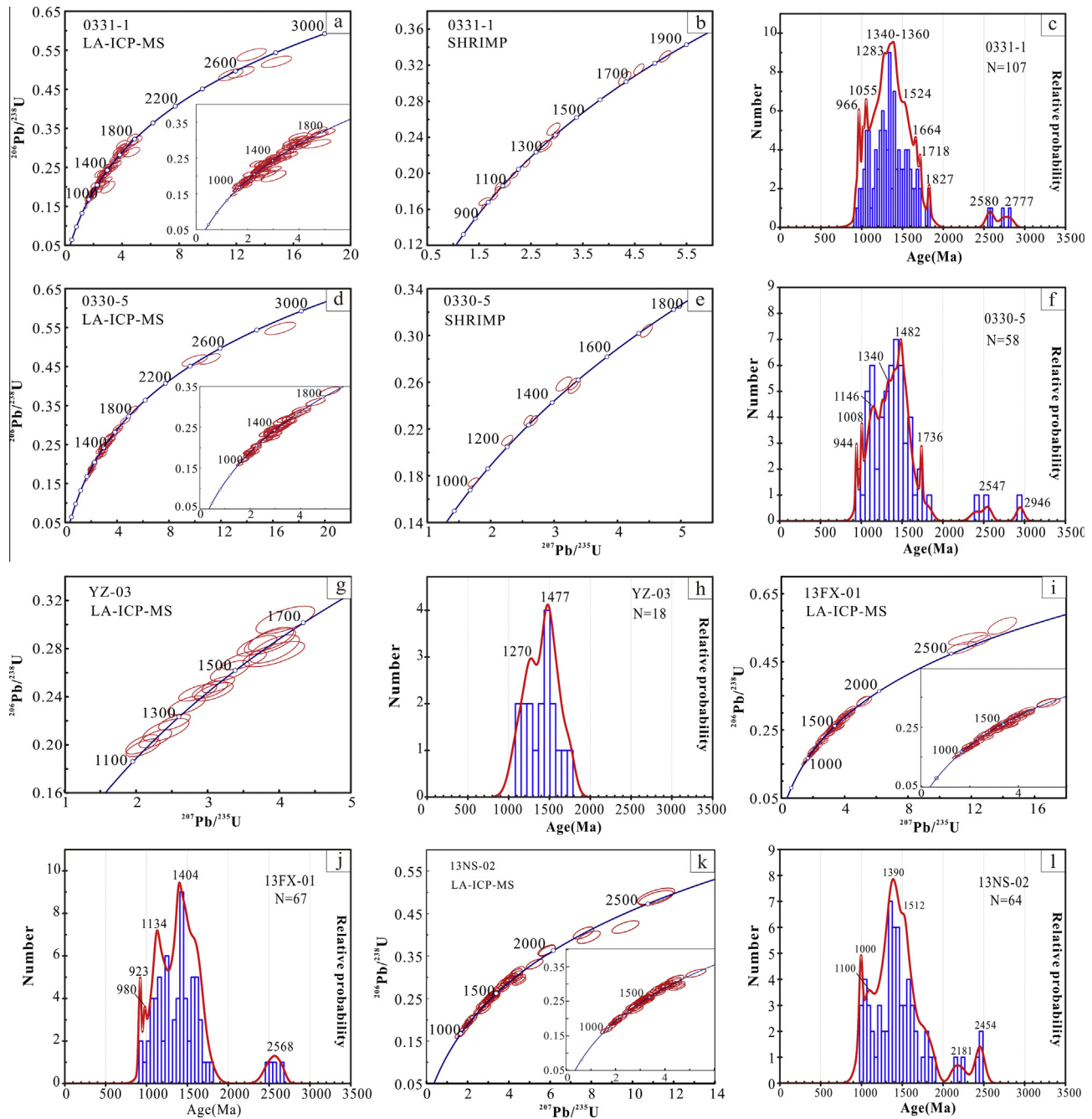
Fig. 4. U–Pb concordia diagrams, isoplot probability density curves and histograms of zircon data from both the Shilu Group and the Shihuiding Formation. All of the U–Pb zircon data are plotted on the U–Pb concordia diagrams, but only the concordant to concordant nearly data are analyzed on probability density plots with histograms.

(Cawood et al., 2013b). The zircon U–Pb data listed in Appendices A1 and A2 were plotted on the U–Pb concordia diagrams (Fig. 4). The concordant data are also analyzed as probability density plots with histograms in Fig. 4. It's notable that those analyses using both methods are counted only once in their cumulative probability plots.

4. U–Pb dating results

A total of 643 analyses by LA-ICP-MS (Appendix A1) and 115 analyses by SHRIMP II (Appendix A2) were conducted on detrital zircons from 15 samples. Mineral inclusions and fissures in zircon grains were avoided during analyses. As shown in Fig. 5, most of

the zircon grains either from the Shilu Group or from the Shihuiding Formation have rounded or subrounded morphologies with various extents of abrasion, whereas less than 5% are subangular or angular. Most grains are characterized by oscillatory or fan-shaped zoning in CL images, and have Th/U values greater than 0.1 (Th/U = 0.12–4.17), which is considered to be of magmatic origin (e.g., Hoskin and Schaltegger, 2003). A small number of grains (e.g., spot 1.1 from sample 0331-1 in Fig. 5) are enveloped by the rims, which display homogeneous structure and have Th/U ratios of 0.04–0.73, indicating a metamorphic origin.

Some zircon grains are analyzed by both LA-ICP-MS and SHRIMP methods. The results showed that the LA-ICP-MS U–Pb ages agree well with the SHRIMP ages, with a good correlation (r^2 = 0.9872; Fig. 6). Nevertheless, two of the eighteen LA-ICP-MS
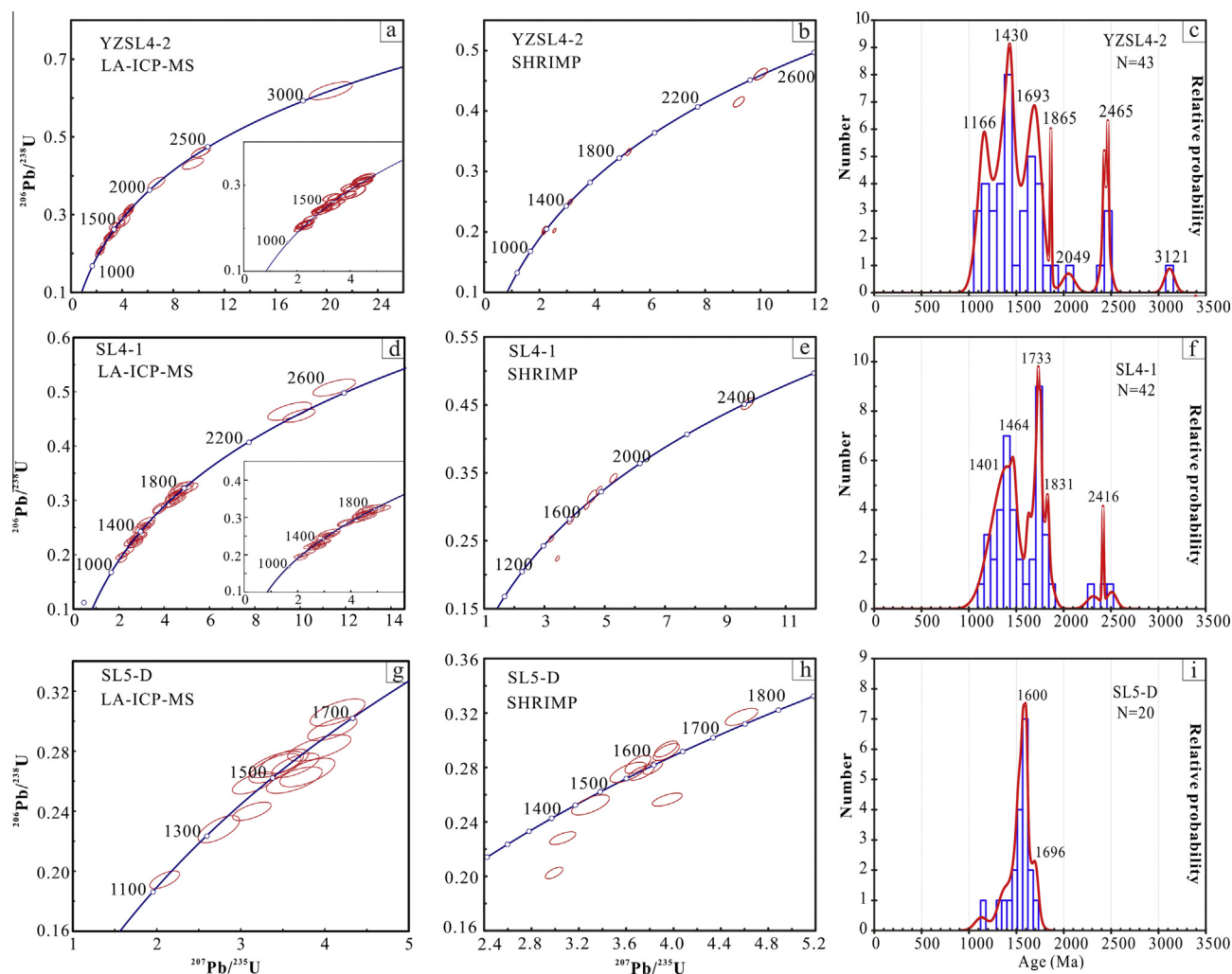
Fig. 4 (*continued*)

ages are inconsistent with SHRIMP ages, i.e. spot 112 with LA-ICP-MS age of 890 ± 9 Ma in sample 0331-1 and spot 04 with LA-ICP-MS age of 889 ± 9 Ma in sample SL-7, which correspond to their SHRIMP ages of 973 ± 11 Ma (spot 6.1) and 933 ± 12 Ma (spot 11.1), respectively. The difference likely results from the fact that LA-ICP-MS collects sample material from a greater depth (10–30 μm) than SHRIMP (less than 1 μm) and thus, would be inclined to obtain "mixed" ages by analyzing other younger zircon domains. In this case, SHRIMP ages should be adopted.

4.1. The Shihuiding Formation

A total of five ferruginous quartz sandstone samples from the Shihuiding Formation were analyzed, including samples 0331-1 and 0330-5 by both SHRIMP II and LA-ICP-MS methods, and YZ-03, 13FX-01 and 13NS-02 by LA-ICP-MS. A total of 116 analyses were performed on 107 grains from sample 0331-1 (Appendices A1 and A2), with 1 rejected due to discordance. These detrital zircons yield a predominant age population between 1700 Ma and 1000 Ma (Fig. 4Aa–c), with one main peak at 1360–1340 Ma, and two subordinate peaks at ca. 1280 Ma and ca. 1055 Ma. There is also a weak cluster between 2830 Ma and 2570 Ma produced by four late Mesoarchean to Neoarchean zircon grains (spots 19, 52, 85 and 104). Four youngest grains were identified, giving $^{206}Pb/^{238}U$ ages of 932 ± 15 Ma (spot 48), 958 ± 10 Ma (spot 3),

969 ± 12 Ma (spot 79) and 973 ± 11 Ma (spot 6.1), respectively. The grain of metamorphic origin yield an age of 1035 Ma (spot 1.1 in Fig. 5). Sixty-one analyses on 58 zircon grains from sample 0330-5 (Appendices A1 and A2) fall within the range of 2950–940 Ma, with one dominant age peak at 1480–1340 Ma, and one subordinate peak at 1150–1050 Ma (Fig. 4Ad–f). One zircon grain (spot 56) with black, faintly fine oscillatory zoning in CL imaging yielded a LA-ICP-MS $^{206}Pb/^{238}U$ age of 941 ± 11 Ma. The narrow metamorphic rim exhibited an age of 1038 Ma (spot 1.1 in Fig. 5) younger than the core of 1194 Ma (spot 63).

Eighteen zircon grains from sample YZ-03 were analyzed, yielding 18 concordant to nearly concordant ages ranging from ca. 1750 Ma to ca. 1080 Ma (Appendix A1), with one predominant age peak at ca. 1480 Ma (Fig. 4Ag–h). A total of 68 analyses were carried out from sample 13FX-01 (Appendix A1). The age population is characterized by a main peak at ca. 1400 Ma, and one subordinate peak at ca. 1135 Ma (Fig. 4Ai–j). Two youngest grains yielded $^{206}Pb/^{238}U$ ages of 928 ± 12 Ma (spot 48) and 911 ± 14 Ma (spot 79), respectively. The metamorphic rim with low Th/U ratio of 0.07 exhibited an age of 1124 Ma (spot 54, Fig. 5) younger than the core of 1261 Ma (spot 53). Sixty-four LA-ICP-MS analyses from samples 13NS-02 (Appendix A1) define one predominant age peak at 1510–1400 Ma (Fig. 4Ak–l). Two youngest ages of 981 ± 19 Ma (spot 34) and 999 ± 17 Ma (spot 42) are also confirmed in this sample.
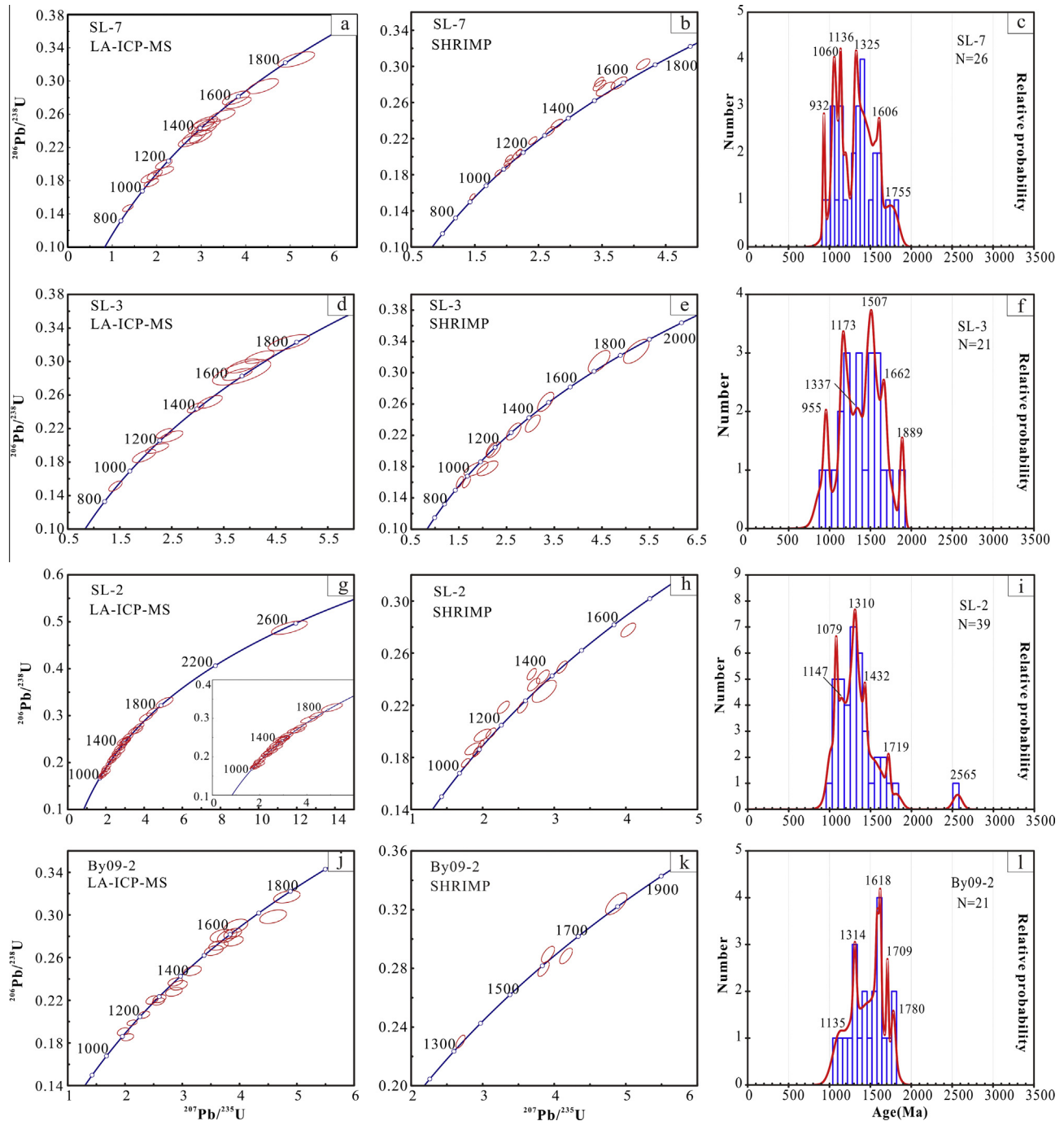
Fig. 4 (*continued*)

4.2. The Shilu Group

4.2.1. The Fourth member

Detrital zircon grains from samples YZSL4-2 (metamorphogenic quartzite) and SL4-1 (metamorphogenic mica-rich quartzite) in the Fourth member of the Shilu Group yielded 45 and 46 analyses by both SHRIMP II and LA-ICP-MS methods, respectively (Appendices A1 and A2). However, two analyses from both samples were rejected, owing to their discordance. The concordant to nearly concordant ages from sample YZSL4-2 define a broad range from 3120 Ma to 1120 Ma (Fig. 4Ba–c), which produced a dominant cluster between 1700 Ma and 1100 Ma, with one main peak at ca. 1430 Ma and two subordinate peaks at ca. 1690 Ma and ca.

1170 Ma. Furthermore, five analyses yielded a less important age cluster between 2500 Ma and 2050 Ma enclosing a minor peak at ca. 2465 Ma. This sample also contains the spot 40 with the oldest age of 3117 ± 53 Ma. Detrital zircons from sample SL4-1 yielded a wide age range from 2510 Ma to 1100 Ma (Appendices A1 and A2), with a predominant age cluster between 1850 Ma and 1100 Ma, which displayed two main peaks at ca. 1730 Ma and 1465–1400 Ma (Fig. 4Bd–f). A less important age cluster between 2510 Ma and 2310 Ma is also present in this sample.

4.2.2. The Fifth member

A total of 24 zircon grains in quartz–mica schist sample SL5-D were measured by both SHRIMP II and LA-ICP-MS methods
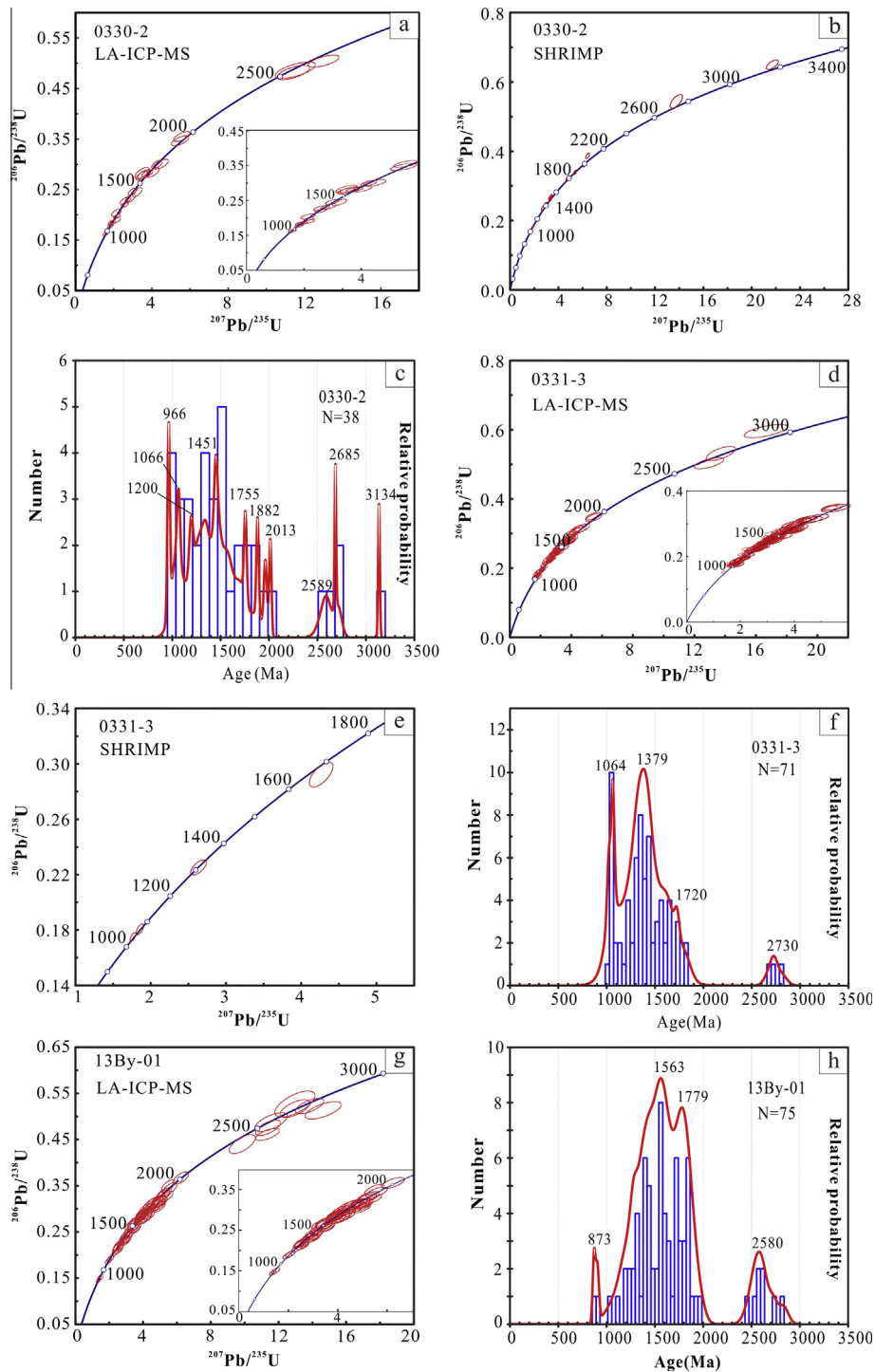
Fig. 4 (*continued*)

(Appendices A1 and A2). However, only 21 ages were concordant to nearly concordant (Fig. 4Bg–h), which yielded a main cluster between 1710 Ma and 1340 Ma with one predominant peak at ca. 1600 Ma (Fig. 4Bi). The youngest grain (spot 9) with euhedral, fractured prism in shape and clearly oscillatory zoning in CL imaging gave a late Mesoproterozoic age of 1140 ± 67 Ma.

4.2.3. The Sixth member
4.2.3.1. Pyroxene–amphibole-rich rocks. The majority of zircon grains from samples SL-7 and SL-3 display concentric or fine oscillatory zoning, and high but variable Th/U values ranging from 0.20

to 1.63 (Appendices A1 and A2). Thirty-three analyses for 29 grains from sample SL-7 were obtained by both SHRIMP II and LA-ICP-MS methods (Appendices A1 and A2). Except for two rejected due to discordance, the others plot on or near the concordia (Fig. 4Ca–b), yielding an age range from 1810 Ma to 930 Ma with two main age peaks at ca. 1325 Ma and 1136–1060 Ma (Fig. 4Cc). A youngest age of 933 ± 12 Ma (spot 11.1) was obtained in this sample. A total of thirty-three analyses from sample SL-3 (Appendices A1 and A2) were obtained by both SHRIMP II and LA-ICP-MS methods, with two rejected due to discordance (Fig. 4Cd–e). These detrital zircons have ages ranging from 1890 Ma to 890 Ma, which present two
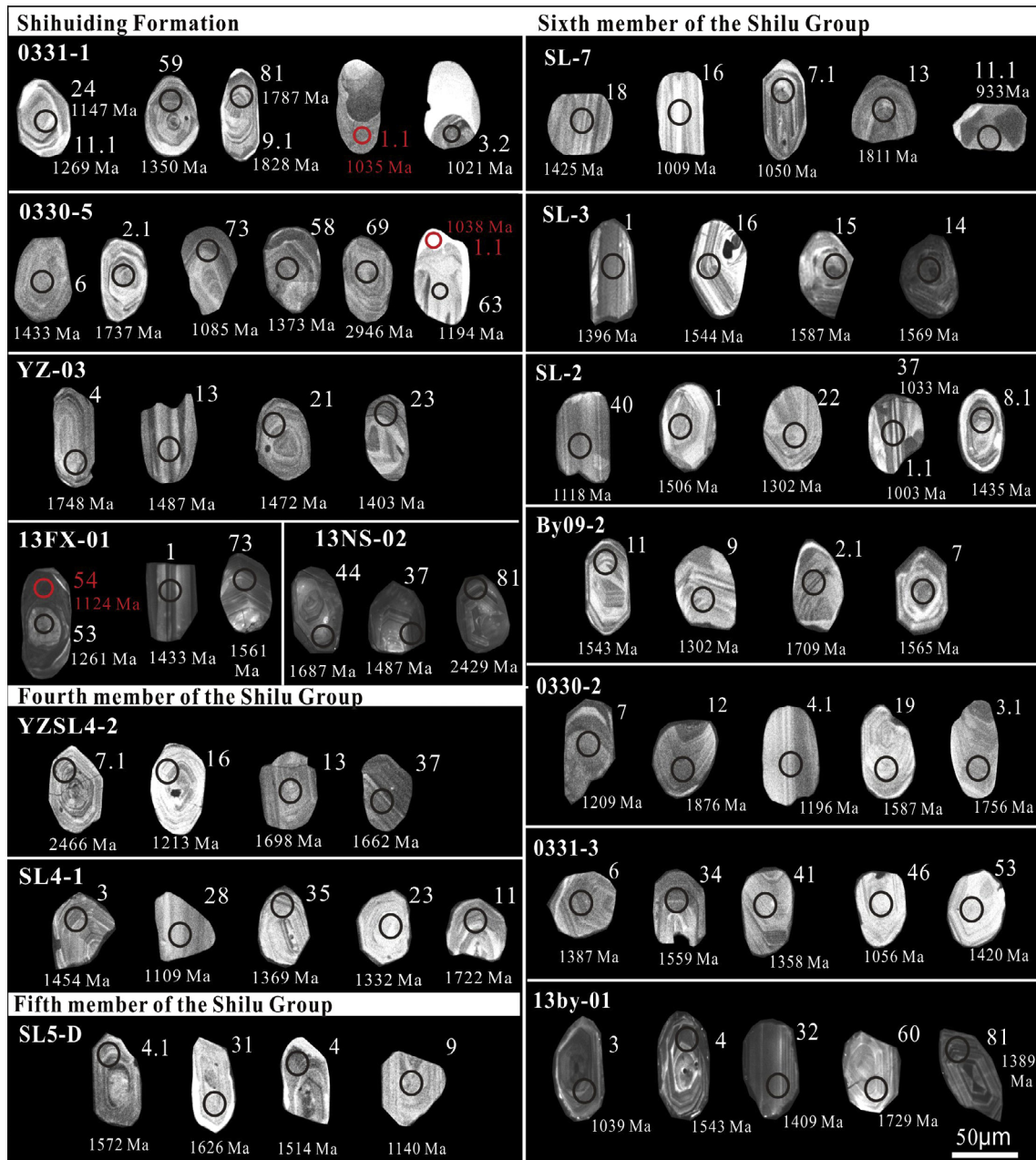
Fig. 5. Representative cathodoluminescence images of detrital zircons from both the Shilu Group and the Shihuiding Formation. Each analyzed spot on zircon grains is marked by a solid circle and corresponding serial number and age value. Serial numbers marked by decimals were analyzed by LA-ICP-MS, whereas the ones marked by integers were analyzed by SHRIMP. The black circle represents the magma-derived zircon and red circle represents metamorphogenic zircon. (For interpretation of the references to colour in this figure legend, the reader is referred to the web version of this article.)

main peaks at ca. 1507 Ma and ca. 1173 Ma (Fig. 4Cf). Two youngest zircon grains (spots 6.1 and 11) yielded two early Neoproterozoic ages at 958 ± 27 Ma and 898 ± 13 Ma, respectively.

4.2.3.2. Fe-poor ores (i.e. amphibolitic itabirites). A total of 48 analyses from sample SL-2 were performed by both LA-ICP-MS and SHRIMP II methods (Appendices A1 and A2). Except for four data discarded due to discordance, the remainder yielded an age range from 2560 Ma to 1000 Ma (Fig. 4Cg–i). The age spectrum consists of a predominant cluster between 1660 Ma and 1035 Ma, with two main age peaks at ca. 1310 Ma and ca. 1080 Ma. Twenty-five analyses on 21 detrital zircons from sample By09-2 by both LA-ICP-MS and SHRIMP II methods yield a narrow age range from 1780 Ma to 1050 Ma (Appendices A1 and A2; Fig. 4Cj–l), which

define one main age peak at ca. 1618 Ma and one subordinate age peak at ca. 1315 Ma. Three youngest grains (spots 4, 13 and 14) with subhedral to xenomorphic morphologies and clearly or faintly fine oscillatory zoning in CL imaging also gave late Mesoproterozoic ages of 1169 ± 69 Ma, 1117 ± 56 Ma and 1054 ± 69 Ma, respectively (Appendices A1 and A2).

4.2.3.3. Phyllites. Forty analyses from sample 0330-2 by both SHRIMP II and LA-ICP-MS methods (Appendices A1 and A2) yielded a broad age range from Mesoarchean to early Neoproterozoic (Fig. 4Da–c). The age spectrum is dominated with a main cluster between 2010 and 960 Ma, with one smaller cluster between 2558 and 2710 Ma. Two main age peaks at 1451–1340 Ma and 1070–970 Ma are present. Two youngest zircons respectively gave
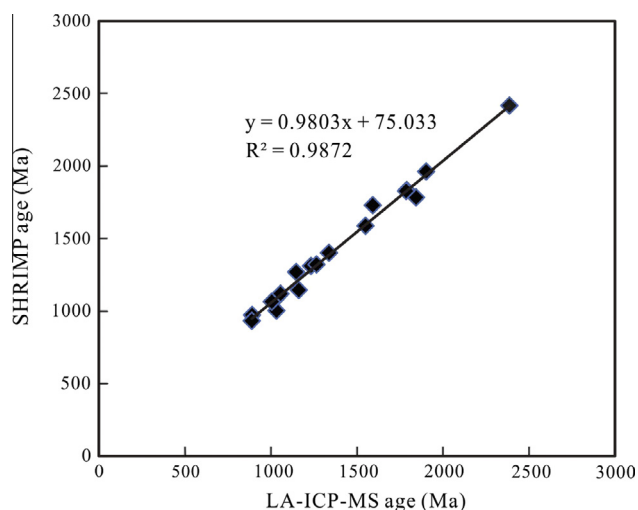
Fig. 6. The diagram of LA-ICP-MS vs. SHRIMP U–Pb ages.

^{206}Pb/^{238}U ages of 967 ± 11 Ma (spot 28) and 959 ± 12 Ma (spot 5.1), whereas the oldest grain (spot 9.1) yielded a Mesoarchean age of 3135 ± 9 Ma.

Seventy-two concordant or nearly concordant U–Pb age data were obtained from sample 0331-3 by both SHRIMP II and LA-ICP-MS methods. They predominantly scatter between 1740 and 1030 Ma (Appendices A1 and A2), with two main peaks at ca. 1380 Ma and ca. 1065 Ma (Fig. 4Dd–f). Three older ages of 2805 ± 56 Ma, 2731 ± 36 Ma and 2681 ± 49 Ma on three zircon grains of magmatic origin yielded a smaller cluster between 2810 and 2680 Ma, with a peak at 2733 Ma.

4.2.3.4. Fe-rich ores (i.e. quartz itabirites). Seventy-five analyses were carried out in sample 13by-01 by LA-ICP-MS method (Appendix A1), which define two age populations at 1970–870 Ma and 2830–2470 Ma (Fig. 4Dg–h). The predominant age population of 1970–870 Ma gave two major peaks at ca. 1780 Ma and ca. 1560 Ma, whereas the less important yielded a main peak at ca. 2580 Ma. Two youngest grains marked by spots 17 and 80 gave ages of 870 ± 13.8 and 905 ± 16.5, respectively.

5. Discussion

5.1. Can the Shihuiding Formation be ascribed to the Shilu Group?

The integrated SHRIMP and LA-ICP-MS analyses, as well as the SHRIMP U–Pb age data from Li et al. (2008a), reveal that detrital zircon grains from the Shihuiding Formation yield a main age range from 1900 to 900 Ma, with a subordinate range from 3000 to 2000 Ma (Fig. 7a). The zircon ages are dominated by a major age peak at 1485–1330 Ma, and three subordinate peaks at 1736–1666 Ma, 1226 Ma and 1013 Ma (Fig. 7a). The detrital zircon grains from the Sixth member of the Shilu Group have a predominant age population between 2000 Ma and 900 Ma, with a small cluster ranging from 2700 Ma to 2500 Ma (Fig. 8a). These age populations define two main peaks at 1440–1320 Ma and 1070 Ma, and two subordinate peaks at 1710–1585 Ma and 1210 Ma. Despite a predominant cluster between 1800 Ma and 1100 Ma, the detrital zircon ages from the Fifth member of the Shilu Group show a main age peak at ca. 1600 Ma (Fig. 8b). With together minor age population at 3200–2000 Ma, the majority of the detrital zircon ages from the Fourth member of the Shilu Group cluster between 1900 Ma and 1100 Ma, which yield two main age peaks at 1730 Ma and 1435 Ma, and one subordinate peak at 1175 Ma (Fig. 8c). As a result, the detrital zircon grains from the Shilu
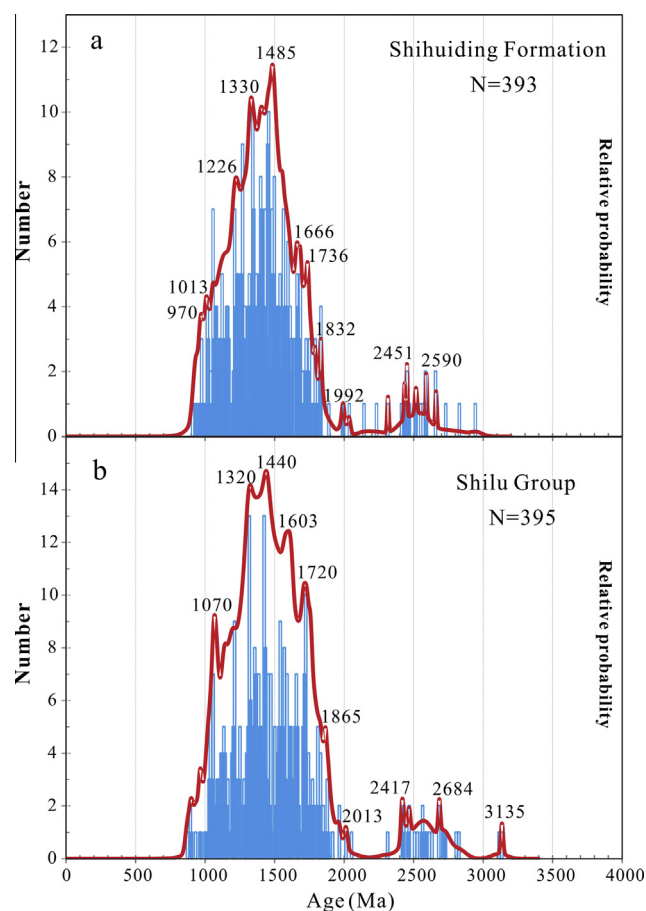

Fig. 7. Isoplot probability density curves and histograms of zircon data from both the Shihuiding Formation (a) and Shilu Group (b).

Group are characterized by a predominant age cluster between 2000 Ma and 900 Ma, and a minor population between 2900 Ma and 2300 Ma, which yield one main peak at 1440–1320 Ma, and three subordinate peaks at 1720 Ma, ca. 1600 Ma and 1070 Ma (Fig. 7b).

The detrital zircon U–Pb age distributions (Fig. 7) between the Shilu Group and overlying Shihuiding Formation are indistinguishable, suggesting that they are part of the same depositional system. This is consistent with the recognition that the Shihuiding Formation contains a similar megafossil assemblage to the Shilu Group (Yao et al., 1999). Thin-section observation also reveals that the Shihuiding Formation had the same metamorphic grade of greenschist-facies which is defined by the characteristic mineral assemblage and texture (Fig. 3d) with the Shilu Group. The fault contact relationship for both successions (Fig. 3a–c) has been interpreted as a result of the responses to late-stage tectonic activities due to the rheological competency contrast between rock types from both the Shihuiding Formation and the Sixth member of the Shilu Group (Xu et al., 2009). Thus it is reasonable to reinterpret the Shihuiding Formation as the top, i.e. the Seventh member of the Shilu Group. Nevertheless, the slight distinction of age peaks among samples from both the successions can be interpreted as an association with local variations in provenance, exhumation, weathering, paleodrainage and depositional setting.

5.2. Maximum depositional time

Based on SHRIMP U–Pb dating on zircon grains from a tuff sample (00SC70) in the Shilu Group, Li et al. (2008a) suggested an early
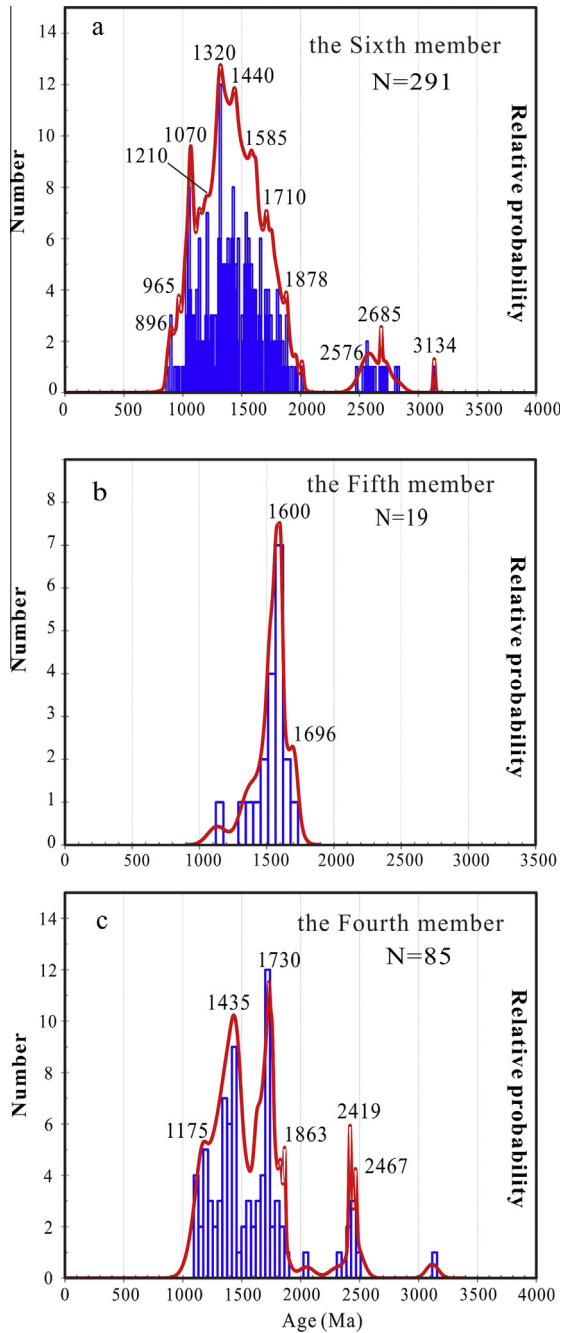
Fig. 8. Isoplot probability density curves and histograms of zircon data from the Sixth (a), Fifth (b) and Fourth (c) members of the Shilu Group.

Mesoproterozoic age of 1439 ± 9 Ma for the Shilu Group sedimentation. However, this age needs to be reconfirmed, as no obvious volcanic component has been recognized in the Shilu district, so far. Although Li et al. (2008a) stated that sample 00SC70 was collected from a volcanic unit of the Shilu Group, the lack of GPS coordinates make it difficult to correlate this sample with Shilu district. Moreover, this age not only agrees within analytical errors with the ca. 1430 Ma age reported for both the Mesoproterozoic granites (Li et al., 2002; Xu et al., 2006) and the Baoban Group complex metavolcaniclastic sample 04HN04 (Li et al., 2008a), but also overlaps with the depositional time-interval of the Baoban Group (1800–1430 Ma). The differentiation in lithology and metamorphic grade between the Shilu Group and the underlying Baoban Group (Fig. 2) suggests distinct sedimentary and tectonic histories,

corresponding to a proposed fault or unconformable contact between both successions (Wang et al., 1991). Therefore, it is unreasonable to interpret the ca. 1440 Ma age as the depositional time of the Shilu Group. Moreover, Li et al. (2008a) reported the SHRIMP zircon U–Pb age data from two Shihuiding Formation samples, which gave the age range from 2661 Ma to 1113 Ma. If concordance is considered, three main age peaks at 1690–1660 Ma, 1485–1440 Ma and 1330–1310 Ma, can be identified. Li et al. (2008a) thus concluded that the Shihuiding Formation was probably a ⩽1200 Ma foreland basin deposit formed during the Grenvillian orogeny. However, detrital zircon grains from the same succession in the present study reveal abundant post-1200 Ma age population, thus suggesting that Li et al. (2008a) had missed the younger age data.

Given that the U–Pb isotope system in detrital zircons remained closed during subsequent hydrothermal, structural-metamorphic and/or magmatic processes, the youngest U–Pb age populations from detrital zircons can be used to constrain maximum depositional time of stratigraphic successions (Kaur et al., 2011 and references therein). The samples from both the Shilu Group and Shihuiding Formation contain abundant detrital zircons with younger, late Mesoproterozoic to early Neoproterozoic ages. A youngest statistical age peak at ca. 1070 Ma has been identified for the Shilu Group (Fig. 7b), which can be interpreted as the maximum depositional time for this Group. Likewise, a youngest statistical age peak at ca. 970 Ma (Fig. 7a) is suggested for the maximum depositional age of the Shihuiding Formation, i.e. the Seventh member of the Shilu Group. Recent chemical U–Th–total-Pb (CHIME) dating results on monazite have also confirmed that the Shilu Group and interbedded BIFs have a depositional time-interval between 1075 Ma and 880 Ma (Xu et al., 2015).

5.3. Provenance

The age spectra of detrital zircons reflect the age distribution of their source rocks, which is the key to identify sediment provenance from unsuspected or eroded sources (e.g., Rainbird et al., 2001). By lateral and stratigraphical comparisons of detrital zircon age spectra in the investigated sedimentary members, variations in the sedimentary source(s) with time can be constrained, and thus reflect the evolution history of the basins (Fonneland et al., 2004). However, it is noted that interpretations of provenance must consider the possible recycling of detritus through sedimentary systems of the same or older age (Dickinson and Gehrels, 2003).

The similar age distributions of detrital zircons from the Shilu Group and the Shihuiding Formation indicate a common provenance for the precursor sediments of both successions. The predominant age peak of 1457–1336 Ma along with two subordinate peaks of 1660 Ma and 1217 Ma in the age population of 1700–1200 Ma (Fig. 9a) most likely corresponds to the prolonged breakup of the Columbia supercontinent during the Mesoproterozoic (e.g., Rogers and Santosh, 2002 and references therein). Detrital zircons with the age cluster of 1700–1200 Ma are widely reported for (meta)sedimentary rocks in both the Yangtze and the Cathaysia Blocks of South China (Fig. 9b and c; Li et al., 2007; Greentree et al., 2006; Wang et al., 2007a, 2010b, 2012a, 2013b, 2014a; Yu et al., 2008, 2010; Sun et al., 2009; Zhou et al., 2009; Wan et al., 2010; Wu et al., 2010; Duan et al., 2011; Yao et al., 2011, 2012; Xu et al., 2012; Cawood et al., 2013b). However, rocks with this age range rarely occurred in the South China, except for the metamorphosed volcanic rocks with ages of ca. 1675 Ma from the Dahongshan Group (Greentree and Li, 2008) in the southwestern part of the Yangtze Block and the 1460 Ma amphibolites from the Yunkai area in the Cathaysia Block (Qin et al., 2006). Rocks with Mesoproterozoic ages have been identified in Hainan Island, including ca. 1433 Ma meta-volcaniclastic rocks in the Baoban complex
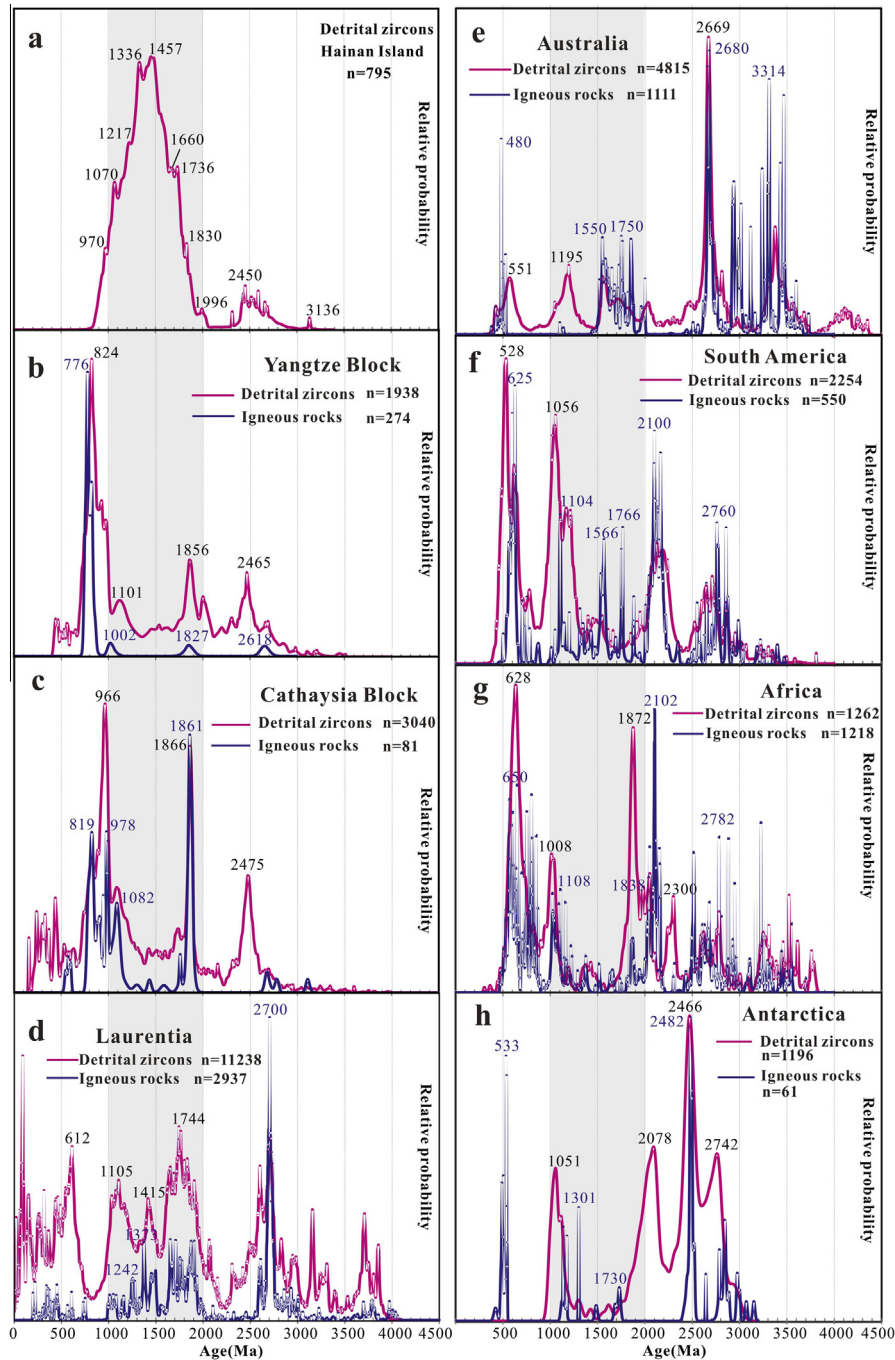
Fig. 9. Probability density plots of U–Pb isotopic ages of detrital and igneous zircons, and their comparisons from Hainan Island (a), Yangtze Block (b), Cathaysia Block (c), Laurentia (d), Australia (e), South America (f), Africa (g), and Antarctica (h). Data are from this study and Li (1999), Li et al. (2002, 2007, 2008a, 2011), Xu et al. (2007a, 2012, 2014b, 2014c), Wan et al. (2007, 2010), Wang et al. (2007a, 2010b, 2012a, 2013b), Shu et al. (2008), Yu et al. (2008), Condie and Aster (2010), Wu et al. (2010), Duan et al. (2011), Yao et al. (2011, 2012) and references therein and in the text.

(Li et al., 2008a) and ca. 1430–1450 Ma gneissic granitoids which intruded into the complex (Ma et al., 1997; Xu et al., 2006; Li et al., 2002, 2008a). Thus the possible provenance for the ca. 1660–1336 Ma detrital zircons from both the Shilu Group and the Shihuiding Formation includes Hainan Island itself or the adjacent continents. The age population of ca. 1900–1200 Ma in both the successions are broadly similar not only to those of Laurentia (Fig. 9d; Ross and Villeneuve, 2003; Thomas et al., 2004; Naipauer et al., 2010; Daniel et al., 2013; May et al., 2013) but also to those in and Australia (Fig. 9e; Berry et al., 2001; Wang et al., 2013b, 2014a). Igneous rocks with the late Paleoproterozoic to middle

Mesoproterozoic ages have also been observed in Laurentia and Australia (Fig. 9d and e), including: (1) igneous rocks of ca. 1800–1600 Ma widespread in both Laurentia (Daniel et al., 2013 and references therein) and Australia (Belousova et al., 2009 and references therein); (2) rocks with ages of ca. 1600–1500 Ma present in Australia (Stewart et al., 2001; Daniel et al., 2013); (3) magmatic rocks of ca. 1500–1300 Ma ages occurring in North America (i.e. central and southern Laurentia; Nyman et al., 1994; Condie et al., 2005), but being absent in Australia (Stewart et al., 2001; Daniel et al., 2013). These suggest a connection between Laurentia, Australia and Hainan Island during this time period.

The Rodinia supercontinent, involving almost all the continents of the world, is thought to have assembled during the time interval from 1300 Ma to 900 Ma (e.g., Hoffman, 1991; Li et al., 2008b). Based on the reconstruction of Li et al. (1995, 1999, 2002, 2008a, 2008b), Hainan Island had been considered to be closer to the Cathaysia Block and was a possible western extension of the southwestern Laurentia before and during the assembly of Rodinia. In the Yangtze Block, granitoids or high-grade metamorphic rocks with Grenville ages are generally absent (Fig. 9b). The only reports include the Grenvillian metamorphism along the SE and the northern to western margins of the Yangtze (e.g., Li et al., 1995, 2002, 2007; Qiu et al., 2000; Wang et al., 2010b, 2012a), and the minor ca. 1100–900 Ma igneous rocks on the western and SE margins of the Yangtze (e.g., Li et al., 2002, 2009a; Greentree et al., 2006; Sun et al., 2009). Likewise, the Grenville-aged rocks are rarely exposed in the Cathaysia (Fig. 9c) except for the ca. 970 Ma rhyolites which contain inherited magmatic zircons with ca. 1100 Ma age in the western Wuyi Mountains (Shu et al., 2008). The general lack of the igneous rocks and associated metamorphic rocks of typical Grenvillian ages (1300–1000 Ma: Boger et al., 2000) in South China is consistent with the following observations: (1) the Yangtze River system without detrital zircons with a predominant age cluster of 1300–1000 Ma (Yang et al., 2012); and (2) the weak age range of 1300–1000 Ma for detrital zircons from the Precambrian basement members and overlying Neoproterozoic sedimentary strata in the Jiangnan Orogen or the SE margin of Yangtze (Wang et al., 2007a, 2010b, 2012b). Therefore, the lack of 1300–1000 Ma magmatism in the South China (Wang et al., 2010b), which is one of the most important events along the continental margins of Australia and Laurentia during the assembly of Rodinia (Veevers et al., 2005; Naipauer et al., 2010 and references therein), rules out the possibility that the 1300–1000 Ma zircons came from the Cathaysia Block. The abundant Mesoproterozoic and especially Stenian (1200–1000 Ma) detrital zircons likely constrain the source rocks of both the Shilu Group and the Shihuiding Formation to be predominantly the 1200–1000 Ma Grenvillian orogeny-related magmatic and metamorphic rocks, such as these in the Grenvillian belts between the eastern Laurentia and its southwestern Amazonia (Fig. 9f; the Rondonia-Sunsas Belt: Hoffman, 1991; Chew et al., 2008), the Grenvillian-Sveconorwegian belts between Laurentia and Baltica (1200–1000 Ma; McAteer et al., 2010; Bingen et al., 2011 and references therein), the Namaqua-Natal Province of Kalahari craton (1130–1070 Ma, Fig. 9g), the Windmill Island in Bunger Hills of northeastern Antarctica (1300–1050 Ma) and the Maud belt of western Antarctica (1300–1070 Ma) (Fig. 9h), and the Wilks-Albany-Fraser belt in Australia (1300–1050 Ma) (Fitzsimons, 2000a, 2000b, 2003; Will et al., 2009 and references therein). Further the detrital zircon ages of ca. 1170–1070 Ma (Fig. 9a) from both the Shilu Group and the Shihuiding Formation are consistent with ca. 1135–1070 Ma granite plutons in central Texas and the ca. 1190 Ma Grenvillian basement in the southern Appalachians (Carrigan et al., 2003; Tollo et al., 2006), along the southern Laurentian margin. Collectively, detrital zircon ages from both the Shilu Group and the Shihuiding Formation are similar to that observed in Laurentia and Australia, especially the Laurentia (Fig. 9d and e), implying the possible continents such as Australia and Laurentia as the potential provenance during the assembly of Rodinia.

5.4. Depositional setting

The morphology and age structure of the present detrital zircons suggest that both the Shilu Group and the Shihuiding Formation were deposited in a relatively stable basinal environment during the late Mesoproterozoic to early Neoproterozoic. The dominance of abraded zircons over angular zircons argues against a proximal source and implies a more stable tectonic setting for deposition of the host rocks and interbedded BIFs. The dominant shallow-water mixed deposition of dolostones and siliciclastics from both the Shilu Group and the Shihuiding Formation favors such a stable depositional environment (Yao et al., 1999). The highly scattered ages for either the abraded or angular detrital zircons (Figs. 7 and 8) also indicate that they were not autogenic, but rather allogenic. This contradicts with the recognition that in situ intensive volcanic or plutonic activities were responsible for genesis of the Shilu district (Fang et al., 1992). Moreover, the volcanic suites, located far to the north of the Shilu district, have been regarded as either Silurian, Carboniferous or Permian (for a review see Xu et al., 2007b). Consequently, the minor amounts of angular zircons with Precambrian ages indicate little near-source debris inputs from volcanic rocks or continental basement, implying a tectonically stable setting, such as a foreland basin (Dickinson and Suczek, 1979). Such a tectonic setting is also consistent with the terrigenous geochemical affinities of the host rocks and interbedded BIFs (Xu et al., 2014a) which indicate a lack of juvenile materials related to intensive crust-scale tectonism in adjacent areas. This corresponds to the present U–Pb age spectra which show only minor amounts of detrital zircons with ages approximating the depositional time of the sediments, suggesting a foreland basin setting formed during continental collision (Cawood et al., 2013a).

The successions and occurrences of the Shilu Group and overlying Shihuiding Formation are consistent with the features of foreland basins described by Burke et al. (1986) and Ravikant et al. (2011), which can be summarized as follows: (1) the transverse cross section of both successions is wedge-shaped, thickest in the SEE section and taping toward NWW (Fig. 1b; also see Fig. 4d in Xu et al., 2013), consistent with the occurrence of most foreland basins (Castle, 2001); (2) the sedimentary facies of both successions changes from neritic fine-grained siliciclastics intercalated with thin carbonate (the First to Fifth members of the Shilu Group), through neritic-thalassic impure carbonate intercalated with siliciclastics (the Sixth member of the Shilu Group), to shoreline-channelized fluvial sandstone (the Shihuiding Formation; Fig. 2), typical of foreland basin deposition (Castle, 2001); (3) there was no contemporaneous magmatic activity; and (4) both successions are defined by two major ductile shear zones, i.e. E-trending Changjiang-Qionghai and NE-trending Gezhen (Fig. 1b) with dipping to the S and dipping to the NW, respectively, similar to most of foreland basins defined by thrust belts or ductile shear zones (DeCelles and Giles, 1996). Thus both the Shilu Group and Shihuiding Formation may be considered to be deposited in a foreland basin. However, minor angular zircons indicate a nearby less active orogenic setting, such as continental arc systems, including peripheral foreland basins, retro-arc foreland basins, or even incipient back-arc basins (Dickinson and Suczek, 1979). Unfortunately, the detrital zircons alone cannot discriminate between these settings. The presence of possible detrital pyroxene and muscovite in the Fourth member of the Shilu Group (Xu et al., 2009) excludes the long-distance transport or episodes of sediment recycling as well as the varied provenances for our studied successions, but indicates the tectonic setting of retro-arc foreland basin (Fig. 10) with the depositional provenance directly from the orogen (e.g., Raines et al., 2013). This is consistent with the metamorphogenic zircons of the main age population of 1200–1000 Ma (Fig. 5) that are indistinguishable in age from the magma-derived zircons of equivalent age, suggesting a high-grade provenance with mixed magmatic/metamorphic zircon growth during this time (e.g., Rainbird et al., 2001).

Under the retro-arc foreland basin, the question remains as to whether the abraded zircons were shed from the sedimentary successions on the uplifted arcs, from the sedimentary covers on the positive topographies within the Hainan Island itself, or from
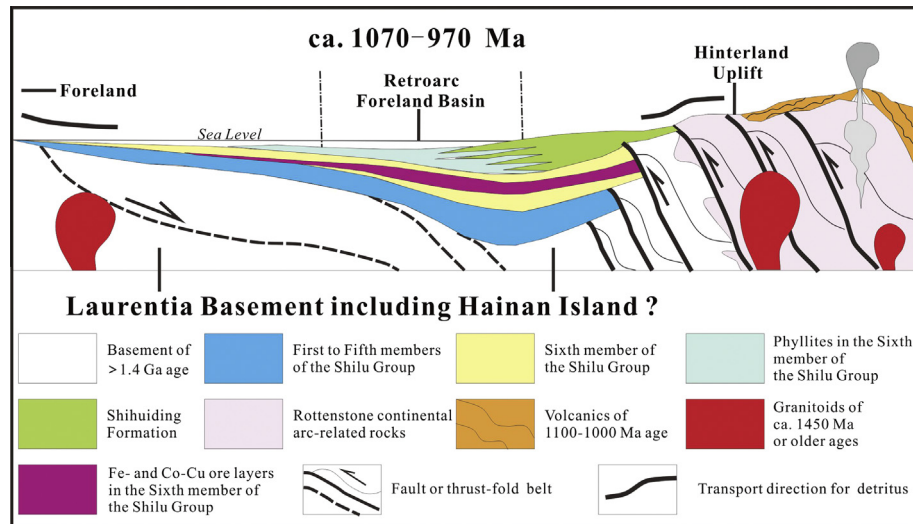
Fig. 10. A suggested retro-arc foreland basin model for deposition of the Shilu Group and overlying Shihuiding Formation related to arc–continent collision tectonic development of Hainan Island.

remote sources. As discussed above, the typical Grenvillian ages (ca. 1300–1000 Ma) for detrital zircons from both the Shilu Group and the Shihuiding Formation indicate their derivation from Laurentia and/or Australia. Based on detailed work in the Grenville province of North America, Rivers (1997) proposed that the Grenville orogeny actually comprised several distinct accretion and collisional events at a Mesoproterozoic convergent margin, including arc accretion at 1250–1190 Ma and pulses of tectonism during protracted continental collision at 1190–1140 Ma, 1080–1020 Ma, and 1000–980 Ma (Fitzsimons, 2003). The detrital zircons from both the Shilu Group and the Shihuiding Formation also reveal the presence of three age populations at 1217–1140 Ma, 1070 Ma, and 970 Ma (Fig. 9a). Given that Hainan Island was still attached to Laurentia during or shortly after the Grenvillian orogeny, it is possible that a retro-arc foreland basin received detritus from an unknown, uplifted orogen comprising a continental magmatic arc and older basement and sediments for deposition of the host rocks and interbedded BIFs in Shilu district (Fig. 10). This is supported by the geochemical affinities of back-arc basalts for the metamorphosed mafic volcanic rocks from the Baoban Group, which in return suggest the presence of a late Paleoproterozoic to Mesoproterozoic arc system (Xu et al., 2002) before the deposition of the Shilu Group. A similar scenario also has been described by Ross and Villeneuve (2003) for the 1470–1400 Ma Mesoproterozoic Belt basin in western North America.

5.5. Position of Hainan Island in Rodinia

Hainan Island was generally considered to be the southernmost extent of the Cathaysia Block (Li et al., 1995, 2002, 2008a, 2008b), therefore, reconstructions of Rodinia supercontinent generally placed it as part of the Cathaysia Block. Previous studies have compared the Jiangnan Orogen between the Cathaysia and the Yangtze Blocks (Fig. 1a) with the Grenvillian orogenic belts in other continents to suggest possible interrelationship between South China and its circumjacent blocks. Consequently, different models have been proposed for the position of South China in the Rodinia: one model suggesting that South China was situated between western Laurentia and southeastern Australia (Li et al., 1995, 2002, 2008a, 2008b; Li et al., 2014), whereas others proposing that the South China was located on the periphery of Rodinia near western Australia

and India (Duan et al., 2011 and references therein; Zhao and Cawood, 2012; Cawood et al., 2013b). Yu et al. (2008, 2010) have also argued that the South China lay adjacent to India and East Antarctica (northern Gondwana) during the period from the breakup of Rodinia to assembly of Gondwana.

However, the above-mentioned models still need to be re-evaluated as to how they relate to the reconstruction of Hainan, because it is debated as to whether Hainan Island was the southern extension of the Cathaysia Block. Xu et al. (2001) argued the crystalline basement of Hainan Island not being part of the southern extension of the Cathaysia Block. Furthermore, Zhang et al. (2014) proposed that the Nanhai terrane (including the Hainan massif) could be the missing link between South China and the Gondwana supercontinent, with the Zhenghe-Dapu fault as the suture zone between South China and the Nanhai terrane. Xu et al. (2014b) suggested that Sanya Block on Hainan Island was separated from mainland South China (including the Qiongzhong Block, Hainan Island) until early to mid-Ordovician and that the juxtaposition of South China and West Australian cratons represented the final assembly of Gondwana. The previous researches have revealed the distinct tectonothermal events between Hainan Island and the South China. Mesoproterozoic igneous rocks only occur in Hainan Island (Li et al., 2002, 2008a; Xu et al., 2006), whereas the Neoproterozoic granites and bimodal volcanic rocks are widespread in the Cathaysia and Yangtze (including the Jiangnan Orogen) Blocks (Li et al., 2008b and references therein; Shu et al., 2011). Unlike those occurring widely in the South China (e.g., Wan et al., 2007, 2010; Wang et al., 2007b, 2010a; Xu et al., 2012; Zhao and Cawood, 2012), the absence of late Ordovician-early Devonian granitic plutons (mainly ca. 450–400 Ma) as well as the rarity of Caledonian (ca. 460–420 Ma) tectonothermal events (Xu et al., 2007a, 2007b) imply that Hainan Island might have been an independent paleoplate at least before the late Ordovician. The lack of Neoproterozoic glaciogenic sediments on Hainan Island, which are widespread in the Yangtze Block (Zhang et al., 2011), also suggests a difference in paleogeography and climate between Hainan and the Yangtze block during this period (Yao et al., 1999). Collectively, these suggest that the late Mesoproterozoic to early Neoproterozoic rocks in Hainan Island might be remnants of a larger old continental domain, whose fragments were preserved in adjacent blocks of the Grenvillian orogenic belt.

Even if Hainan Island was the southern extension of the Cathaysia Block, it still remains controversial whether the Jiangnan Orogen could be considered as a Grenvillian orogeny. Generally, the assembly of the Yangtze and Cathaysia Blocks was considered to have taken place at 1000–900 Ma (e.g., Guo et al., 1985), or at 960–860 Ma (e.g., Zheng et al., 2008), or at ca. 880 Ma or soon after (Li et al., 2009b). Greentree et al. (2006) suggested that the Yangtze and Cathaysia Blocks amalgamated in the west at ca. 1180–1140 Ma and finally assembled at 1000–960 Ma, whereas Li et al. (2007) proposed a collision time of 1042–1015 Ma for the western part and 970–920 Ma for the eastern part. Based on the presence of the two distinctive peaks of ca. 1170 Ma and ca. 970 Ma for detrital zircons from the SE Yangtze Block, Yao et al. (2012) proposed that the Grenville orogeny in the South China was multi-stage. However, Wang et al. (2014b) proposed that the assembly of the Yangtze with the Cathaysia Blocks took place after 825 Ma, consistent with the previous consideration that the amalgamation of the two Blocks was not completed until ca. 820 Ma or even later (see Li et al., 2011 for a review). In addition, Yu et al. (2008) showed that ocean subduction under the Yangtze Block occurred at ca. 882 Ma, and a continent (Yangtze)-arc collision occurred after 824 Ma. Similarly, the slab-arc model of Zhao et al. (2011) proposed that the Yangtze and Cathaysia Blocks were fused to form the Jiangnan Orogen at ca. 830 Ma. U–Pb isotopic data for detrital zircons from northeastern Guizhou and Guangxi seem to support the assembly at 860–800 Ma (Wang et al., 2007a; Zhou et al., 2009). Abundant Grenville-aged (1050–900 Ma) detrital zircons have been found in Precambrian metasedimentary rocks along the western margin of the Yangtze, and the Zengcheng and Xunwu gneiss in the southern part of the Cathaysia (Sun et al., 2009 and references therein). This distribution suggests that the western and southwestern Yangtze (e.g., the Panxi-Hannan belt of Zhao and Cawood, 2012) and southeastern Cathaysia (Yao et al., 2011, 2012) were likely close to some parts of the Grenvillian orogen, respectively. However, the suggested Grenville-aged orogens in South China are younger by ca. 300–100 Ma even 560–300 Ma (Sun et al., 2009) than the typical Grenvillian orogen in Texas, the Albany-Fraser and Musgrave orogeny in central Australia and the Grenville Province in southern

Laurentia, but similar to the Eastern Ghats (ca. 960 Ma) in India and Northern Prince Charles Mountains (990–960 Ma) in East Antarctica. Li et al. (1995, 2002) proposed the "Missing-Link" model in which the South China (including Hainan) was located between Australia-East Antarctica and Laurentia. However, Wang et al. (2007a) queried on this model due to the selected samples in Li et al. (2002) from neither the interior nor areas near the suture between the Yangtze and Cathaysia Blocks, but from Hainan Island. The detrital zircon population with typical Grenvillian ages (ca. 1300–1000 Ma) for both the Shilu Group and the Shihuiding Formation (Fig. 9a) suggests that Hainan Island was derived from Grenville orogen(s) neither in the Yangtze and Cathaysia Blocks nor in the Eastern Ghat and East Antarctica, but adjacent to western Laurentia and central Australia (1300–1050 Ma) or to one part of Laurentia (Fig. 11). Therefore, the present study supports the reconstruction of South China on the periphery of Rodinia, and suggests that Hainan Island was likely located on an unknown Grenville-aged orogen adjacent to western Laurentia and close to eastern Australia (Fig. 11).

6. Conclusion

Detrital zircons from the Shilu Group and the overlying Shihuiding Formation in the Shilu BIF-type Fe–Co–Cu ore district, Hainan Province of South China, display consistent age spectra and predominantly cluster between 2000 and 900 Ma. Combined with the lithological, mineralogical, structural and paleontological evidence, the geochronology of detrital zircons suggest the same depositional system for both successions, and thus the Shihuiding Formation can be re-interpreted as the top, i.e. the Seventh member of the Shilu Group. The youngest statistical zircon age peaks of both successions may define the maximum depositional time of the Shilu Group and interbedded BIF ore source rocks as the late Mesoproterozoic to early Neoproterozoic (ca. 1070–970 Ma).

Most of the present detrital zircons show rounded or sub-rounded morphologies. At least two sources are proposed: one distal or recycled to provide abraded zircons and the other proximal to provide least abraded zircons. The dominance of abraded zircon grains over angular ones, as well as the distinction in zircon U–Pb age spectrum between Hainan and South China indicate a relatively stable tectonic setting for depositions of both the Shilu Group and Shihuiding Formation with precursor sediments dominantly from Laurentia and subordinately from Australia. Combined with the comparison of the Jiangnan Orogen (880–740 Ma) in South China with the worldwide, typical Grenvillian orogens, the Precambrian plate tectonics of Laurentia or Gondwana suggest that the Shilu Group and interbedded BIF-type Fe–Co–Cu ore source rocks were deposited in a retro-arc foreland basin developed on western Laurentia during the assembly of Rodinia. Linked to the lack of the Neoproterozoic-early Paleozoic granites and the Neoproterozoic glaciogenic sediments, as well as the presence of the Mesoproterozoic granites, the present study implies that Hainan Island likely was independent of South China at least before the late Ordovician.
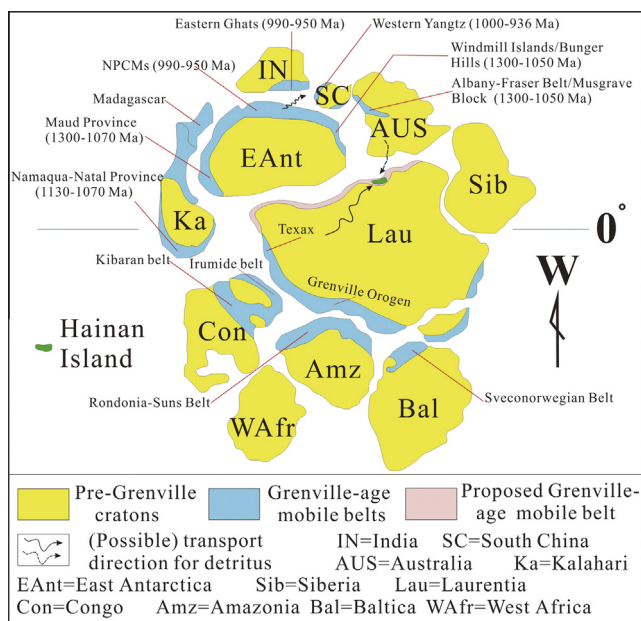
Fig. 11. Possible positions of South China and Hainan Island in Rodinia, modified after Hoffman (1991) and Fitzsimons (2000a, 2000b, 2003).

reviewers for their thorough and constructive reviews, and Guest Editor M. Santosh for editorial handling of the paper.

Appendix A. Supplementary material

Supplementary data associated with this article can be found, in the online version, at http://dx.doi.org/10.1016/j.jseaes.2015.04.014.

References

Andersen, T., 2002. Correction of common lead in U–Pb analyses that do not report [204]Pb. Chem. Geol. 192 (1), 59–79.

Belousova, E.A., Reid, A.J., Griffin, W.L., O'Reilly, S.Y., 2009. Rejuvenation vs. recycling of Archean crust in the Gawler Craton, South Australia: evidence from U–Pb and Hf isotopes in detrital zircon. Lithos 113, 570–582.

Berry, R.F., Jenner, G.A., Meffre, S., Tubrett, M.N., 2001. A North American provenance for Neoproterozoic to Cambrian sandstones in Tasmania? Earth Planet. Sci. Lett. 192, 207–222.

Bingen, B., Belousova, E.A., Griffin, W.L., 2011. Neoproterozoic recycling of the Sveconorwegian orogenic belt: detrital-zircon data from the Sparagmite basins in the Scandinavian Caledonides. Precambr. Res. 189, 347–367.

Boger, S.D., Carson, C.J., Wilson, C.J.L., Fanning, C.M., 2000. Neoproterozoic deformation in the Radok Lake region of the northern Prince Charles Mountains, east Antarctica: evidence for a single protracted orogenic event. Precambr. Res. 104, 1–24.

Burke, K., Kidd, W.S.F., Kusky, T.M., 1986. Archean foreland basin tectonics in the Witwatersrand, South Africa. Tectonics 5, 439–456.

Carrigan, C., Miller, C., Fullagar, P., Bream, B., Hatcher Jr., R.D., Coath, C., 2003. Ion microprobe age and geochemistry of southern Appalachian basement, with implications for Proterozoic and Paleozoic reconstructions. Precambr. Res. 120, 1–36.

Castle, J.W., 2001. Appalachian basin stratigraphic response to convergent–margin structural evolution. Basin Res. 13, 397–418.

Cawood, P.A., Hawkesworth, C.J., Dhuime, B., 2013a. Detrital zircon record and tectonic setting. Geology 40, 875–878.

Cawood, P.A., Wang, Y.J., Xu, Y.J., Zhao, G.C., 2013b. Locating South China in Rodinia and Gondwana: a fragment of greater India lithosphere? Geology 41, 903–906.

Chew, D.M., Magna, T., Kirkland, C.L., Mišković, A., Cardona, A., Spikings, R., Schaltegger, U., 2008. Detrital zircon fingerprint of the Proto-Andes: evidence for a Neoproterozoic active margin? Precambr. Res. 167, 186–200.

Condie, K.C., Aster, R.C., 2010. Episodic zircon age spectra of orogenic granitoids: the supercontinent connection and continental growth. Precambr. Res. 180, 227–236.

Condie, K.C., Beyer, E., Belousova, E., Griffin, W.L., O'Reilly, S.Y., 2005. U–Pb isotopic ages and Hf isotopic composition of single zircons: the search for juvenile Precambrian continental crust. Precambr. Res. 139, 42–100.

Daniel, C.G., Pfeifer, L.S., Jones III, J.V., McFarlane, C.M., 2013. Detrital zircon evidence for non-Laurentian provenance, Mesoproterozoic (ca. 1490–1450 Ma) deposition and orogenesis in a reconstructed orogenic belt, northern New Mexico, USA: defining the Picuris orogeny. Geol. Soc. Am. Bull. 125, 1423–1441.

DeCelles, P.G., Giles, K.N., 1996. Foreland basin systems. Basin Res. 8, 105–123.

Dickinson, W.R., Gehrels, G.E., 2003. U–Pb ages of detrital zircons from Permian and Jurassic eolian sandstones of the Colorado Plateau, USA: paleogeographic implications. Sed. Geol. 163, 29–66.

Dickinson, W.R., Suczek, C.A., 1979. Plate tectonics and sandstone compositions. Am. Assoc. Petrol. Geol. Bull. 63, 2164–2182.

Duan, L., Meng, Q.R., Zhang, C.L., Liu, X.M., 2011. Tracing the position of the South China block in Gondwana: U–Pb ages and Hf isotopes of Devonian detrital zircons. Gondwana Res. 19, 141–149.

Fang, Z., Zhao, J.X., McCulloch, M.T., 1992. Geochemical and Nd isotopic study of Paleozoic bimodal volcanics in Hainan Island, South China – implications of rifting tectonics and mantle reservoirs. Lithos 29, 127–139.

Fedo, C.M., Sircombe, K.N., Rainbird, R.H., 2003. Detrital zircon analysis of the sedimentary record. Rev. Mineral. Geochem. 53, 277–303.

Fitzsimons, I.C.W., 2000a. A review of tectonic events in the East Antarctic Shield, and their implications for Gondwana and earlier supercontinents. J. Afr. Earth Sc. 31, 3–23.

Fitzsimons, I.C.W., 2000b. Grenville-age basement provinces in East Antarctica: evidence for three separate collisional orogens. Geology 28, 879–882.

Fitzsimons, I.C.W., 2003. Proterozoic basement provinces of southern and southwestern Australia, and their correlation with Antarctica. In: Yoshida, M., Windley, D.F., Dasgupta, S. (Eds.), Proterozoic East Gondwana: Supercontinent Assembly and Breakup, vol. 206. Geological Society, Special Publications, London, pp. 93–130.

Fonneland, H.C., Lien, T., Martinsen, O.J., Pedersen, R.B., Kosler, J., 2004. Onshore and offshore provenance studies: a key to understanding the deposition of deep marine sandstones in the Norwegian Sea. Sed. Geol. 164, 147–159.

Gerdes, A., Zeh, A., 2006. Combined U–Pb and Hf isotope LA-(MC-)ICP-MS analyses of detrital zircons: comparison with SHRIMP and new constraints for the provenance and age of an Armorican metasediment in Central Germany. Earth Planet. Sci. Lett. 249, 47–61.

Greentree, M.R., Li, Z.X., 2008. The oldest known rocks in south-western China: SHRIMP U–Pb magmatic crystallisation age and detrital provenance analysis of the Paleoproterozoic Dahongshan Group. J. Asian Earth Sci. 33, 289–302.

Greentree, M.R., Li, Z.X., Li, X.H., Wu, H.C., 2006. Late Mesoproterozoic to earliest Neoproterozoic basin record of the Sibao orogenesis in west South China and relationship to the assembly of Rodinia. Precambr. Res. 151, 79–100.

Guo, Z., Shi, Y.S., Ma, R.S., Lu, H.F., Ye, S.F., 1985. Plate movement and crustal evolution of the Jiangnan Proterozoic mobile belt, SE China. Earth Sci. J. Geol. Soc. Jpn. 2, 156–166.

HBGMR (Hainan Bureau of Geology and Mineral Resources), 1997. Lithostratigraphy of Hainan Province. Chinese University of Geosciences Press, Wuhan, pp. 1–125 (in Chinese).

Hoffman, P.F., 1991. Did the breakout of Laurentia turn Gondwanaland inside out? Science 252, 1409–1412.

Hoskin, P.W.O., Schaltegger, U., 2003. The composition of zircon and igneous and metamorphic petrogenesis. In: Hanchar, J.M., Hoskin, P.W.O. (Eds.), Zircon. Reviews in Mineralogy and Geochemistry. The Mineralogical Society of America, Washington, pp. 27–62.

Kaur, P., Zeh, A., Chaudhri, N., Gerdes, A., Okrusch, M., 2011. Archaean to Palaeoproterozoic crustal evolution of the Aravalli mountain range, NW India, and its hinterland: The U–Pb and Hf isotope record of detrital zircon. Precambr. Res. 187, 155–164.

Li, X.H., 1999. U–Pb zircon ages of granites from the southern margin of the Yangtze margin: timing of Neoproterozoic Jinning Orogen in SE China and implication for Rodinia assembly. Precambr. Res. 97, 43–57.

Li, Z.X., Zhang, L., Powell, C.M.A., 1995. South China in Rodinia: part of the missing link between Australia-East Antarctica and Laurentia? Geology 23, 407–410.

Li, Z.X., Li, X.H., Kinny, P.D., Wang, J., 1999. The breakup of Rodinia: did it start with a mantle plume beneath South China? Earth Planet. Sci. Lett. 173, 171–181.

Li, Z.X., Li, X.H., Zhou, H.W., Kinny, P.D., 2002. Grenvillian continental collision in South China: new SHRIMP U–Pb zircon results and implications for the configuration of Rodinia. Geology 30, 163–166.

Li, Z.X., Wartho, J.A., Occhipinti, S., Zhang, C.L., Li, X.H., Wang, J., Bao, C.M., 2007. Early history of the eastern Sibao Orogen (South China) during the assembly of Rodinia: new mica [40]Ar/[39]Ar dating and SHRIMP U–Pb detrital zircon provenance constraints. Precambr. Res. 159, 79–94.

Li, Z.X., Li, X.H., Li, W.X., Ding, S.J., 2008a. Was Cathaysia part of Proterozoic Laurentia? – new data from Hainan Island, south China. Terra Nova 20, 154–164.

Li, Z.X., Bogdanova, S.V., Collins, A.S., Davidson, A., De Waele, B., Ernst, R.E., Fitzsimons, I.C.W., Fuck, R.A., Gladkochub, D.P., Jacobs, J., Karlstrom, K.E., Lu, S., Natapov, L.M., Pease, V., Pisarevsky, S.A., Thrane, K., Vernikovsky, V., 2008b. Assembly, configuration, and break-up history of Rodinia: a synthesis. Precambr. Res. 160, 179–210.

Li, X.H., Li, W.X., Li, Z.X., Lo, Q.H., Wang, J., Ye, M.F., Yang, Y.H., 2009a. Amalgamation between the Yangtze and Cathaysia Blocks in South China: constraints from SHRIMP U–Pb zircon ages, geochemistry and Nd-Hf isotopes of the Shuangxiwu volcanic rocks. Precambr. Res. 174, 117–128.

Li, Z.X., Li, X.H., Wartho, J.A., Clark, C., Li, W.X., Zhang, C.L., Bao, C.M., 2009b. Magmatic and metamorphic events during the Early Paleozoic Wuyi-Yunkai Orogeny, southeastern South China: new age constraints and P–T conditions. Geol. Soc. Am. Bull. 122, 772–793.

Li, L.M., Sun, M., Wang, Y.J., Xing, G.F., Zhao, G.C., He, Y.H., He, K.J., Zhang, A.M., 2011. U–Pb and Hf isotopic study of detrital zircons from the metasedimentary rocks in central Jiangxi Province, South China: implications for the Neoproterozoic tectonic evolution of South China Block. J. Asian Earth Sci. 41 (1), 44–55.

Li, X.H., Li, Z.X., Li, W.X., 2014. Detrital zircon U–Pb age and Hf isotope constrains on the generation and reworking of Precambrian continental crust in the Cathaysia Block, South China: a synthesis. Gondwana Res. 25, 1202–1215.

Ludwig, K., 2001a. SQUID, Version 1.02: A Geochronological Toolkit for Microsoft Excel. Berkeley Geochronology Center, Special Publication, No. 2, pp. 19.

Ludwig, K.R., 2001b. Users Manual for Isoplot/Ex (rev. 2.49): A Geochronological Toolkit for Microsoft Excel. Berkeley Geochronology Center, Special Publication, No. 1a, pp. 56.

Ma, D.Q., Wang, X.D., Chen, Z.P., Xiao, Z.F., Zhang, W.C., Zhong, S.Z., 1997. New achievements about Baoban Group in Hainan Island. Regional Geol. China 16 (2), 130–136 (in Chinese with English abstract).

May, S.R., Gray, G.G., Summa, L.L., Stewart, N.R., Gehrels, G.E., Pecha, M.E., 2013. Detrital zircon geochronology from the Bighorn Basin, Wyoming, USA: implications for tectonostratigraphic evolution and paleogeography. Geol. Soc. Am. Bull. 125, 1403–1422.

McAteer, C.A., Daly, J.S., Flowerdew, M.J., Connelly, J.N., Housh, T.B., Whitehouse, M.J., 2010. Detrital zircon, detrital titanite and igneous clast U–Pb geochronology and basement–cover relationships of the Colonsay Group, SW Scotland: Laurentian provenance and correlation with the Neoproterozoic Dalradian Supergroup. Precambr. Res. 181, 21–42.

Naipauer, M., Vujovich, G.I., Cingolani, C.A., McClelland, W.C., 2010. Detrital zircon analysis from the Neoproterozoic-Cambrian sedimentary cover (Cuyania terrane), Sierra de Pie de Palo, Argentina: evidence of a rift and passive margin system? J. S. Am. Earth Sci. 29, 306–326.

Nelson, D.R., 2001. An assessment of the determination of depositional ages for Precambrian clastic sedimentary rocks by U–Pb dating of detrital zircons. Sed. Geol. 141–142, 37–60.

Nyman, M.W., Karlstrom, K.E., Kirby, E., Graubard, C.M., 1994. Mesoproterozoic contractional orogeny in western North America: evidence from ca 1.4 Ga plutons. Geology 22, 901–904.

Qin, X.F., Pan, Y.M., Li, J., Li, R.S., Hu, G.A., Zhong, F.Y., 2006. Zircon SHRIMP U–Pb geochronology of the Yunkai metamorphic complex in southeastern Guangxi, China. Geol. Bull. China 25, 553–559.

Qiu, Y.M., Gao, S., McNaughton, N.J., Groves, D.I., Ling, W.L., 2000. First evidence of >3.2 Ga continental crust in the Yangtze craton of south China and its implications for Archean crustal evolution and Phanerozoic tectonics. Geology 28, 11–14.

Rainbird, R.H., Hamilton, M.A., Young, G.M., 2001. Detrital zircon geochronology and provenance of the Torridonian, NW Scotland. J. Geol. Soc. 158, 15–27.

Raines, M.K., Hubbard, S.M., Kukulski, R.B., Leier, A.L., Gehrels, G.E., 2013. Sediment dispersal in an evolving foreland: detrital zircon geochronology from Upper Jurassic and lowermost Cretaceous strata, Alberta Basin, Canada. Geol. Soc. Am. Bull. 125, 741–755.

Ravikant, V., Wu, F.Y., Ji, W.Q., 2011. U–Pb age and Hf isotopic constraints of detrital zircons from the Himalayan foreland Subathu sub-basin on the Tertiary palaeogeography of the Himalaya. Earth Planet. Sci. Lett. 304, 356–368.

Rivers, T., 1997. Lithotectonic elements of the Grenville Province: review and tectonic implications. Precambr. Res. 86, 117–154.

Rogers, J.J.W., Santosh, M., 2002. Configuration of Columbia, a Mesoproterozoic Supercontinent. Gondwana Res. 5, 5–22.

Ross, G.M., Villeneuve, M., 2003. Provenance of the Mesoproterozoic (1.45 Ga) Belt basin (western North America): another piece in the pre-Rodinia paleogeographic puzzle. Geol. Soc. Am. Bull. 115, 1191–1217.

SCISTCAS (South China Iron-rich Scientific Team, Chinese Academy of Sciences), 1986. Geology of Hainan Island and Geochemistry of Iron Ore Deposits in Shilu. Science Press, Beijing, pp. 1–376 (in Chinese).

Shu, L.S., Deng, P., Yu, J.H., Wang, Y.B., Jiang, S.Y., 2008. The age and tectonic environment of the rhyolitic rocks on the western side of Wuyi Mountain, South China. Sci. China, Ser. D: Earth Sci. 38, 950–959.

Shu, L.S., Faure, M., Yu, J.H., Jahn, B.M., 2011. Geochronological and geochemical features of the Cathaysia block (South China): new evidence for the Neoproterozoic breakup of Rodinia. Precambr. Res. 187, 263–276.

Stewart, J.H., Gehrels, G.E., Barth, A.P., Link, P.K., Christie-Blick, N., Wrucke, C.T., 2001. Detrital zircon provenance of Mesoproterozoic to Cambrian arenites in the western United States and northwestern Mexico. Geol. Soc. Am. Bull. 113, 1343–1356.

Sun, W.H., Zhou, M.F., Gao, J.F., Yang, Y.H., Zhao, X.F., Zhao, J.H., 2009. Detrital zircon U–Pb geochronological and Lu–Hf isotopic constraints on the Precambrian magmatic and crustal evolution of the western Yangtze Block, SW China. Precambr. Res. 172, 99–126.

Thomas, W.A., Astini, R.A., Muller, P.A., Gehrels, G.E., Wooden, J.L., 2004. Transfer of the Precordillera terrane from Laurentian: constraints from detrital-zircon geochronology. Geology 32, 965–968.

Tollo, R.P., Aleinikoff, J.N., Borduas, E.A., Dickin, A.P., McNutt, R.H., Fanning, C.M., 2006. Grenvillian magmatism in the northern Virginia Blue Ridge: petrologic implications of episodic granitic magma production and the significance of postorogenic A-type charnockite. Precambr. Res. 151, 224–264.

Veevers, J.J., Saeed, A., Belousova, E.A., Griffin, W.L., 2005. U–Pb ages and source composition by Hf-isotope and trace-element analysis of detrital zircons in Permian sandstone and modern sand from southwestern Australia and a review of the paleogeographical and denudational history of the Yilgarn Craton. Earth Sci. Rev. 68, 245–279.

Wan, Y.S., Liu, D.Y., Xu, M.H., Zhuang, J.M., Song, B., Shi, Y.R., Du, L.L., 2007. SHRIMP U–Pb zircon geochronology and geochemistry of metavolcanic and metasedimentary rocks in Northwestern Fujian, Cathaysia Block, China: tectonic implications and the need to redefine lithostratigraphic units. Gondwana Res. 12, 166–183.

Wan, Y.S., Liu, D.Y., Wilde, S.A., Cao, J.J., Chen, B., Dong, C.Y., Song, B., Du, L.L., 2010. Evolution of the Yunkai Terrane, South China: evidence from SHRIMP zircon U–Pb dating, geochemistry and Nd isotope. J. Asian Earth Sci. 37, 140–153.

Wang, X.F., Ma, D.Q., Jiang, D.H., 1991. Geology of Hainan Island: Stratum and Paleo-biology. Geology Publishing House, Beijing, pp. 7–32 (in Chinese).

Wang, X.L., Zhou, J.C., Griffin, W.L., Wang, R.C., Qiu, J.S., O'Reilly, S.Y., Xu, X.S., 2007a. Detrital zircon geochronology of Precambrian basement sequences in the Jiangnan orogen: dating the assembly of the Yangtze and Cathaysia Blocks. Precambr. Res. 159, 117–131.

Wang, Y.J., Fan, W.M., Zhao, G.C., Ji, S.C., Peng, T.P., 2007b. Zircon U–Pb geochronology of gneissic rocks in the Yunkai massif and its implications on the Caledonian event in the South China Block. Gondwana Res. 12, 404–416.

Wang, L.J., Griffin, W.L., Yu, J.H., O'Reilly, S.Y., 2010a. Precambrian crustal evolution of the Yangtze Block tracked by detrital zircons from Neoproterozoic sedimentary rocks. Precambr. Res. 177, 131–144.

Wang, Y.J., Zhang, F., Fan, W., Zhang, G., Chen, S., Cawood, P.A., Zhang, A., 2010b. Tectonic setting of the South China Block in the early Paleozoic: resolving intracontinental and ocean closure models from detrital zircons. Tectonics 29, TC6020.

Wang, L.J., Yu, J.H., Griffin, W.L., O'Reilly, S.Y., 2012a. Early crustal evolution in the western Yangtze Block: evidence from U–Pb and Lu–Hf isotopes on detrital zircons from sedimentary rocks. Precambr. Res. 222–223, 368–385.

Wang, X.C., Li, X.H., Li, Z.X., Li, Q.L., Tang, G.Q., Gao, Y.Y., Zhang, Q.R., Liu, Y., 2012b. Episodic Precambrian crust growth: evidence from U–Pb ages and Hf–O isotopes of zircon in the Nanhua Basin, central South China. Precambr. Res. 222–223, 386–403.

Wang, Y.J., Fan, W.M., Zhang, G.W., Zhang, Y.H., 2013a. Phanerozoic tectonics of the South China Block: key observations and controversies. Gondwana Res. 23 (4), 1273–1305.

Wang, L.J., Griffin, W.L., Yu, J.H., O'Reilly, S.Y., 2013b. U–Pb and Lu–Hf isotopes in detrital zircon from Neoproterozoic sedimentary rocks in the northern Yangtze Block: implications for Precambrian crustal evolution. Gondwana Res. 23, 1261–1272.

Wang, Q.F., Deng, J., Li, C.S., Li, G.J., Yu, L., Qiao, L., 2014a. The boundary between the Simao and Yangtze blocks and their locations in Gondwana and Rodinia: constraints from detrital and inherited zircons. Gondwana Res. 26, 438–448.

Wang, X.L., Zhou, J.C., Griffin, W.L., Zhao, G.C., Yu, J.H., Qiu, J.S., Zhang, Y.J., Xing, G.F., 2014b. Geochemical zonation across a Neoproterozoic orogenic belt: isotopic evidence from granitoids and metasedimentary rocks of the Jiangnan orogeny, China. Precambr. Res. 242, 154–171.

Will, T.M., Zeh, A., Gerdes, A., Frimmel, H.E., Millar, I.L., Schmäicke, E., 2009. Palaeoproterozoic to Palaeozoic magmatic and metamorphic events in the Shackleton Range, East Antarctica: constraints from zircon and monazite dating, and implications for the amalgamation of Gondwana. Precambr. Res. 172, 25–45.

Williams, I.S., Buick, I.S., Cartwright, I., 1996. An extended episode of early Mesoproterozoic metamorphic fluid flow in the Reynolds Range, central Australia. J. Metamorph. Geol. 14, 29–47.

Wu, L., Jia, D., Li, H.B., Deng, F., Li, Y.Q., 2010. Provenance of detrital zircons from the late Neoproterozoic to Ordovician sandstones of South China: implications for its continental affinity. Geol. Mag. 147, 974–980.

Xu, D.R., Fan, W.M., Liang, X.Q., Tang, H.F., 2001. Characteristics of Proterozoic metamorphic basement in Hainan Island and its implications for crustal growth: Nd and Pb isotope constraints. Geol. J. China Univ. 7 (2), 146–157 (in Chinese with English abstract).

Xu, D.R., Liang, X.Q., Tang, H.F., 2002. Geochemical characteristics of Baoban Group metasedimentary rocks in western Hainan, China. Geochimica 31 (2), 153–160 (in Chinese with English abstract).

Xu, D.R., Xia, B., Li, P.C., Zhang, Y.Q., Chen, G.H., Ma, C., 2006. SHRIMP U–Pb dating of zircons from the Precambrian granitoids in northwest Hainan Island and its geological implications. Geotect. Metall. 30, 510–518 (in Chinese with English abstract).

Xu, D.R., Ma, C., Li, P.C., Xia, B., Zhang, Y.Q., 2007a. U–Pb SHRIMP-dating of zircon domains from metaclastic sedimentary rocks in Hainan Island, South China, and its geological significance. Acta Geol. Sin. 81, 383–391 (in Chinese with English abstract).

Xu, D.R., Xia, B., Li, P.C., et al., 2007b. Protolith natures and U–Pb SHRIMP zircon ages of the metabasites in Hainan Island, South China: implications for geodynamic evolution since the Precambrian. Island Arc 16, 575–597.

Xu, D.R., Xiao, Y., Xia, B., Cai, R.J., Hou, W., Wang, L., Liu, C.L., Zhao, B., 2009. Metallogenic Model and Ore Prediction of the Shilu Iron Ore Deposit in Hainan Province. Geological Publishing House, Beijing, pp. 37–39, pp. 175–176 (in Chinese).

Xu, Y.J., Du, Y.S., Cawood, P.A., Zhu, Y.H., Li, W.C., Yu, W.C., 2012. Detrital zircon provenance of Upper Ordovician and Silurian strata in the northeastern Yangtze Block: response to orogenesis in South China. Sed. Geol. 267–268, 63–72.

Xu, D.R., Wang, Z.L., Cai, J.X., Wu, C.J., Bakun-Czubarow, N., Wang, L., Chen, H.Y., Baker, M.J., Kusiak, M.A., 2013. Geological characteristics and metallogenesis of the Shilu Fe-ore deposit in Hainan Province, South China. Ore Geol. Rev. 53, 318–342.

Xu, D.R., Wang, Z.L., Chen, H.Y., Hollings, P., Jansen, N.H., Zhang, Z.C., Wu, C.J., 2014a. Petrography and geochemistry of the Shilu Fe–Co–Cu ore district, South China: implications for the origin of a Neoproterozoic BIF system. Ore Geol. Rev. 57, 322–350.

Xu, Y.J., Cawood, P.A., Du, Y.S., Zhong, Z.Q., Hughes, N.C., 2014b. Terminal suturing of Gondwana along the southern margin of South China Craton: evidence from detrital zircon U–Pb ages and Hf isotopes in Cambrian and Ordovician strata, Hainan Island. Tectonics 33 (12), 2490–2504.

Xu, Y.H., Sun, Q.G., Cai, G.Q., Yin, X.J., Chen, J., 2014c. The U–Pb ages and Hf isotopes of detrital zircons from Hainan Island, South China: implications for sediment provenance and the crustal evolution. Environ. Earth Sci. 71 (4), 1619–1628.

Xu, D.R., Kusiak, M.A., Wang, Z.L., Chen, H.Y., Bakun-Czubarow, N., Wu, C.J., Konečný, P., Hollings, P., 2015. Microstructural observation and chemical dating on monazite from the Shilu Group, Hainan Province of South China: implications for origin and evolution of the Shilu Fe–Co–Cu ore district. Lithos 216–217, 158–177.

Yang, S.Y., Zhang, F., Wang, Z.B., 2012. Grain size distribution and age population of detrital zircons from the Changjiang (Yangtze) River system, China. Chem. Geol. 296–297, 26–38.

Yao, H.Z., Sheng, X.C., Zhang, R.J., 1999. Neoproterozoic sedimentary environment of Shilu Area, Hainan Island, South China. Gondwana Res. 2, 563–566.

Yao, J.L., Shu, L.S., Santosh, M., 2011. Detrital zircon U–Pb geochronology, Hf-isotopes and geochemistry—new clues for the Precambrian crustal evolution of Cathaysia Block, South China. Gondwana Res. 20, 553–567.

Yao, J.L., Shu, L.S., Santosh, M., Li, J.Y., 2012. Precambrian crustal evolution of the South China Block and its relation to supercontinent history: constraints from U–Pb ages, Lu–Hf isotopes and REE geochemistry of zircons from sandstones and granodiorite. Precambr. Res. 208–211, 19–48.

Yu, J.H., O'Reilly, S.Y., Wang, L.J., Griffin, W.L., Zhang, M., Wang, R.C., Jiang, S.Y., Shu, L.S., 2008. Where was South China in the Rodinia supercontinent? Evidence from U–Pb geochronology and Hf isotopes of detrital zircons. Precambr. Res. 164, 1–15.

Yu, J.H., O'Reilly, S.Y., Wang, L.J., Griffin, W.L., Zhou, M.F., Zhang, M., Shu, L.S., 2010. Components and episodic growth of Precambrian crust in the Cathaysia Block,

South China: evidence from U–Pb ages and Hf isotopes of zircons in Neoproterozoic sediments. Precambr. Res. 181, 97–114.

Zhang, R.J., Feng, S.N., Xu, G.H., Yang, D.L., Yan, D.P., Li, Z.H., Jiang, D.H., Wu, W., 1990. Discovery of Chuaria-Tawuia assemblage in Shilu Group, Hainan Island and its significance. Sci. China 33 (2), 211–220.

Zhang, R.J., Ma, G.G., Feng, S.N., Yan, D.P., 1992. Sm–Nd age of the Shilu iron ore deposits on Hainan Island and its significance. Sci. Geol. Sin. 1, 38–43 (in Chinese with English abstract).

Zhang, Q.R., Chu, X.L., Feng, L.J., 2011. Neoproterozoic glacial records in the Yangtze Region, China. In: Arnaud, E., Halverson, G.P., Shields-Zhou, G. (Eds.), The Geological Record of Neoproterozoic Glaciations, vol. 36. Geological Society, Memoirs, London, pp. 357–366.

Zhang, C.L., Santosh, M., Zhu, Q.B., Chen, X.Y., Huang, W.C., 2014. The Gondwana connection of South China: evidence from monazite and zircon geochronology

in the Cathaysia Block. Gondwana Res. http://dx.doi.org/10.1016/j.gr.2014.09.007.

Zhao, G.C., Cawood, P.A., 2012. Precambrian geology of China. Precambr. Res. 222–223, 13–54.

Zhao, J.H., Zhou, M.F., Yan, D.P., Zheng, J.P., Li, J.W., 2011. Reappraisal of the ages of Neoproterozoic strata in South China: no connection with the Grenvillian orogeny. Geology 39 (4), 299–302.

Zheng, Y.F., Wu, R.X., Wu, Y.B., Zhang, S.B., Yuan, H.L., Wu, F.Y., 2008. Rift melting of juvenile arc-derived crust: geochemical evidence from Neoproterozoic volcanic and granitic rocks in the Jiangnan Orogen, South China. Precambr. Res. 163, 351–383.

Zhou, J.C., Wang, X.L., Qiu, J.S., 2009. Geochronology of Neoproterozoic mafic rocks and sandstones from northeastern Guizhou, South China: coeval arc magmatism and sedimentation. Precambr. Res. 170, 27–42.